BIOLOGICAL ION EXCHANGE FOR REMOVAL OF NATURAL ORGANIC MATTER FROM SURFACE WATER IN LONG-TERM OPERATION

by

Jaycee Lynn Wright

B.A.Sc, The University of British Columbia, 2019

A THESIS SUBMITTED IN PARTIAL FULFILLMENT OF

THE REQUIREMENTS FOR THE DEGREE OF

MASTER OF APPLIED SCIENCE

in

THE FACULTY OF GRADUATE AND POSTDOCTORAL STUDIES

(Chemical and Biological Engineering)

THE UNIVERSITY OF BRITISH COLUMBIA

(Vancouver)

April 2022

© Jaycee Lynn Wright, 2022

The following individuals certify that they have read, and recommend to the Faculty of Graduate and Postdoctoral Studies for acceptance, a thesis entitled:

Biological Ion Exchange for Removal of Natural Organic Matter from Surface Water in Long-Term Operation

submitted by Jaycee Lynn Wright in partial fulfillment of the requirements for

the degree of Master of Applied Science

in Chemical and Biological Engineering

Examining Committee:

Dr. Madjid Mohseni, Chemical and Biological Engineering, UBC
Supervisor

Dr. Susan Baldwin, Chemical and Biological Engineering, UBC
Supervisory Committee Member

Dr. Jonathan Verrett, Chemical and Biological Engineering, UBC
Supervisory Committee Member

Abstract

The ion exchange (IEX) process utilizing anion exchange resin is a promising technology for the removal of natural organic matter (NOM) from surface water. Despite its high efficacy, IEX has a major disadvantage of requiring frequent resin regeneration that produces large volumes of high concentration brine, creating disposal issues. Biological ion exchange (BIEX) is an alternative method of operating an IEX column through primary and secondary IEX into biodegradation of NOM, with the goal of reducing regeneration requirements while still achieving high NOM removal.

This research aimed to explore the efficacy of the BIEX process in the field with high NOM concentration surface source water. It particularly focused on comparing BIEX against common treatment technologies. Two pilot-scale opaque fibreglass columns 167 cm tall, containing approximately 68 and 80 L of Purolite A860 resin and AlamoBrand granular activated carbon respectively, were operated for 466 days. The overall system performance was examined over multiple seasons, which accompanied changes in source water quality. In addition, the impact of different backwashing (water and air scour) was examined. Further, resin aliquots were extracted from the BIEX column and subject to in-lab multiple loading tests to investigate resin capacity changes. Performance of these systems was determined by monitoring the concentrations of dissolved organic carbon and various anions, ultraviolet absorbance of water, turbidity, pH, and temperature.

The BIEX filter effectively removed NOM for 3 months, after which biofilm growth hindered secondary IEX. The BIEX filter life was nearly doubled with an increase in EBCT and implementation of air scour backwash procedures, likely due to the disruption of biofilm and resin aggregates. Resin capacity at pilot scale could be estimated by performing multiple loading

tests on extracted resins, and these tests also showed that biofilm growth may have negatively affected access to sulphate-loaded active sites.

Lay Summary

Natural organic matter (NOM) poses challenges to drinking water treatment, and rural and remote communities face additional challenges, like costly transportation of supplies and lack of economies of scale. Technologies exist for the removal of NOM from drinking water, but these may fail to meet the needs of remote communities. These communities need solutions that are robust and require minimal chemicals or operator intervention. Ion exchange is one such process; however, it produces a waste regeneration brine, creating disposal issues. Biological ion exchange is similar to ion exchange but can operate for much longer, weeks versus days, without regeneration. This allows for NOM removal with significantly less waste production. This research examines the efficiency of NOM removal by biological ion exchange through performing long-term drinking water field experiments in the rural community of Gillies Bay Improvement District.

Preface

This is original and unpublished work performed by J. Wright, under the supervision of Dr. Madjid Mohseni (Chemical and Biological Engineering) at the University of British Columbia. J. Wright's contribution to this work involved the literature review, design and active work on the laboratory and pilot scale experiments, data collection, performing analytical tests, and analysis and presentation of the data. Dr. Mohseni contributed to the development of the experimental plan and the research objectives, and has provided much guidance over the course of this research.

Table of Contents

List of Tables

List of Figures

List of Abbreviations and Symbols

AC	Activated carbon
ANOVA	Analysis of variance
BAC	Biological activated carbon
BDOC	Biodegradable dissolved organic carbon
BDOM	Biodegradable dissolved organic matter
BOC	Biodegradable organic carbon
BOM	Biodegradable organic matter
BIEX	Biological ion exchange
BV	Bed volume
$CaCO_3$	Calcium carbonate
Cl^-	Chloride
CO_2	Carbon dioxide
DBP	Disinfection by-products
DI	Deionized [water]
DOC	Dissolved organic carbon
DWA	Drinking water advisory
EBCT	Empty bed contact time
EEM	Excitation emission matrix
IEX	Ion exchange
GAC	Granular activated carbon
GBID	Gillies Bay Improvement District
HCO_3	Bicarbonate
H_3PO_4	Phosphoric acid
HAA	Haloacetic acids

HCl	Hydrochloric acid
IC	Inorganic Carbon
MLT	Multiple loading test
NaCl	Sodium chloride
Na_2CO_3	Sodium carbonate
$NaHCO_3$	Sodium bicarbonate
$(NH_4)_2S_2O_8$	Ammonium persulphate
NO_3^-	Nitrate
NOM	Natural organic matter
NTU	Nephelometric turbidity units
PAC	Powdered activated carbon
PVDF	Polyvinylidene difluoride
SO_4^{2-}	Sulphate
SUVA	Specific ultraviolet absorbance
TC	Total carbon
THM	Trihalomethanes
TOC	Total organic carbon
UBC	The University of British Columbia
UV	Ultraviolet
UVA_{254}	Ultraviolet absorbance at 254nm
VSS	Volatile suspended solids

Acknowledgements

I wish to thank my supervisor, Dr. Madjid Mohseni, for his thoughtful encouragement, unwavering support, and caring mentorship throughout my graduate studies. I am incredibly grateful to have had his patience and guidance over the last two and a half years as he pushed me to be my best during this incredibly rewarding experience! I also want to thank my committee members, Dr. Susan Baldwin and Dr. Jonathan Verrett, for their time and support on this research and its transition into a graduate project.

I also want to thank my colleagues in the SWIRL laboratory, who have answered my many questions, helped guide me along the way, and have been my marvellous companions during long lab days. I want to particularly thank William Chen, whose assistance greatly contributed to bring this research to where it is now, and for being my partner during long days on site.

I wish to thank the community of Gillies Bay Improvement District, in particular Theresa Beech, administrator, and the water operator, Ken Taylor, for their support and confidence in this project. This thesis wouldn't exist without Ken! Thank you to the Moss Rock Park Foundation, for their financial contribution, and to RESEAU Centre for Mobilizing Innovation, for facilitating the work and making this project possible.

Special thanks to my parents and my husband, for standing beside me as I travel my path and who support me every step of the way.

Dedication

To all who deserve clean water but do not yet have access, I dedicate this work to you.

Chapter 1: Introduction

Natural organic matter (NOM) present in raw drinking water sources can pose quality, aesthetic, and treatment issues. There are treatment technologies available to remove NOM, however the end-user community characteristics must be accounted for when considering a treatment process. For small and remote communities, there are additional barriers to implementing various treatment processes. Technologies that require chemicals, like coagulation and flocculation, are not ideal for these communities due to transportation difficulties reaching these remote areas. Rural and remote communities may have fluctuating populations throughout the year, creating a range of water demands. The costs to purchase, transport, and dispose of chemicals and waste products are another barrier to implementation. For these small remote communities, hence, ideal treatment systems must be robust, requiring minimal chemical use and operator intervention.

Ion exchange (IEX) and biological ion exchange (BIEX) are two technologies that are being explored for use in small and remote communities for drinking water treatment. Ion exchange is an excellent technology for removal of NOM, but it requires weekly regeneration using a high concentration salt brine solution. This spent brine requires proper storage and disposal, which can be a struggle for these communities. However, it has recently come to light that IEX can be described as a combination of two sequential mechanisms: primary IEX and secondary IEX (Zimmermann et al., 2021). Traditionally, regeneration occurs at the end of primary IEX; however, if the resins are not regenerated, NOM removal is still possible through secondary IEX followed by biodegradation: BIEX. Extended operation, through primary IEX, secondary IEX, and biodegradation, have shown that regeneration may be delayed for up to one year (Amini et al., 2018).

To test the efficacy of IEX and BIEX for raw drinking water with high NOM concentration, a mobile pilot plant was transported to a small community on the west coast of British Columbia, where it treated raw water for over one year using IEX, BIEX, granular activated carbon (GAC) and biological activated carbon (BAC). Laboratory experiments were performed at the University of British Columbia Vancouver campus, to explore how regeneration is affected by BIEX resin exhaustion and to examine resin saturation.

This thesis compiles the results obtained over the course of this research, discussing the pilot scale and the laboratory scale results separately in two different chapters. The outline of this thesis is as follows:

Chapter 1: High level overview of the research undertaken for completion of this thesis.

Chapter 2: A comprehensive literature review into the definition of NOM, the difficulties of NOM removal in large and small communities, and treatment methods like GAC, BAC, IEX, and BIEX. An investigation is presented on the difficulties faced for disposal of regeneration brine, and the current knowledge gaps for use of BIEX in NOM removal are numerated.

Chapter 3: Provides the research approach, objectives, and hypotheses to be addressed in this thesis.

Chapter 4: Discusses the methods and procedures used in this research.

Chapter 5: Provides and discusses the results of the pilot study.

Chapter 6: Provides and discusses the results of the laboratory study and compares them to the pilot study results.

Chapter 7: Discusses overall conclusions reached in this research and provides recommendations for future work.

Chapter 2: Background and Literature Review

2.1 Natural Organic Matter (NOM)

Natural organic matter (NOM) is a complex matrix of organic materials found universally in water and soil and is one of the main challenges associated with drinking water treatment. NOM originates from the breakdown of plants, is produced as by-products of biological activity, and can be washed into bodies of water from the soil (Crittiden, 2012; Sillanpää, 2015). NOM differs in its molecular size, composition, and charge density, containing various functional groups like phenolic, amino, and most significantly carboxylic, which give NOM a negative charge at neutral pH as found in drinking water sources (Sillanpää, 2015; Thurman, 1985). NOM composition is affected by seasonal changes in the environment (Sillanpää, 2015). NOM can be categorized into humic acids which are generally larger, and fulvic acids which are more soluble due to a greater number of polar groups per unit (Alkan et al., 2007; Chen et al., 2002; Crittiden, 2012; Sillanpää, 2015). One hypothetical example of the structure of NOM is shown in Figure 2-1.

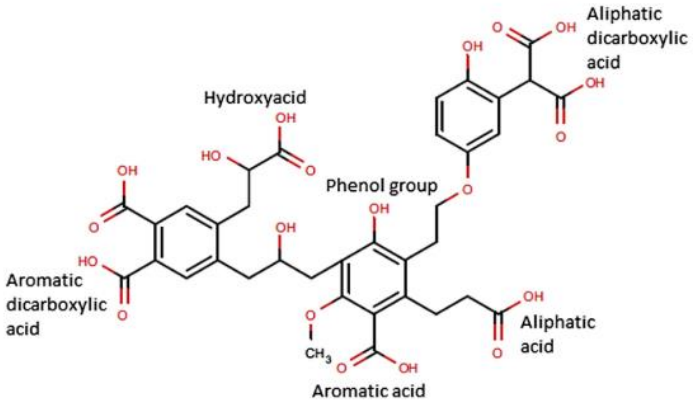

Figure 2-1: A hypothetical structure of one category of NOM, humic acid (Sillanpää, 2015)**.**

The measurements of ultraviolet absorbance at 254nm (UVA_{254}) and total organic carbon (TOC) are surrogate indicators of the amount of NOM in water (Crittiden 2012; Thurman 1985). TOC is further defined and measured as dissolved organic carbon (DOC), which is the fraction of TOC that remains after 0.45 µm filtration, as shown in Figure 2-2 below:

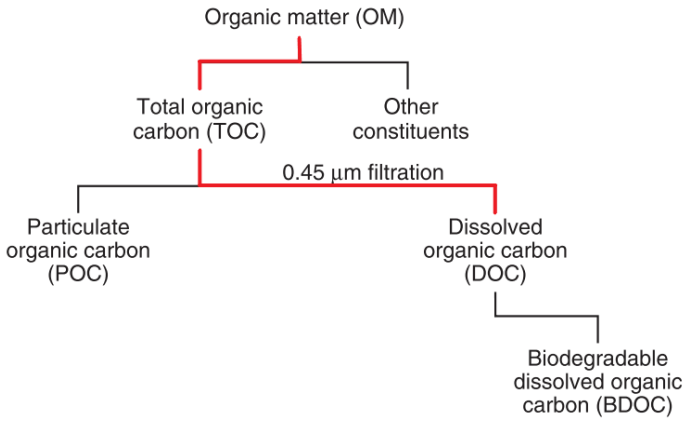

Figure 2-2: Classification of organic matter in water sources as used for drinking water treatment, adapted from (Crittiden, 2012).

DOC is used in this research as a surrogate measurement of NOM, and DOC will be used in subsequent sections when describing treatment performance.

2.2 Water Treatment Challenges Associated with NOM

NOM causes water treatment issues. When using microfiltration or ultrafiltration for water treatment, the presence of NOM causes irreversible fouling through particulate deposition in the filtration membrane pores (Yamamura et al., 2007). When using ultraviolet disinfection, the efficiency is reduced as the DOC present absorbs UV light, and particulate matter protects pathogens by interfering and shading pathogens from UV light (Alkan et al., 2007; Crittiden, 2012; Sillanpää, 2015). NOM is a source of food for bacteria, and causes biofilm growth in

treatment processes and distribution infrastructure (Sillanpää, 2015). NOM also reacts with chemicals like coagulants which are added during the treatment process, increasing the required doses (Crittiden, 2012). NOM further reacts with oxidizing chemicals used for disinfection and forms disinfection by-products (DBPs) like haloacetic acids (HAA) and trihalomethanes (THMs) (Bolto et al., 2002; Crittiden, 2012; Sillanpää, 2015; Thurman, 1985). These DBPs are known to cause a variety of adverse health issues, like bladder cancer, birth defects and premature birth (Cantor et al., 1997; Crittiden, 2012; Kramer et al., 1992; Sillanpää, 2015; Villanueva et al., 2007). Further, the reaction of NOM with disinfectants decreases the pathogen-inactivation potential of the disinfectant, or at minimum requires greater disinfectant dosing. From an aesthetic standpoint, NOM negatively affects the quality of drinking water by causing odour, taste, and colour problems (Crittiden, 2012; Sillanpää, 2014).

2.3 Challenges Faced by Remote Communities

In addition to the difficulties mentioned in section 2.2 when treating NOM in drinking water, treatment systems required by rural and remote communities face further challenges. The need for sustainable water treatment systems in such rural communities is highlighted by the number of long- and short-term drinking water advisories (DWAs) seen in Canada. As of August 2021, 50 long-term DWAs and over 900 combined short- and long-term DWAs were in place in Canada (Government of Canada, 2021; WaterToday, 2021). Between 2010 and 2019, an average 98% of DWAs were in communities with 5000 people or less, and 100% of the long-term DWAs in place were in Indigenous communities (Government of Canada, 2020, 2021). Rural communities are those with populations below 1000 people (Statistics Canada, 2022). These communities may be located along active logging roads which may be impassable in the winter

months or require access by boat. With the loss of economies of scale due to small populations, difficulties in chemical and maintenance supplies transportation, and lack of trained maintenance and operations personnel, treatment facilities in these locations need to be tailored to fit the needs of the community. Treatment systems that require regular chemical or supplies shipments, like coagulation and flocculation or membrane filtration treatments, may be a poor fit for remote communities. An optimal system for these communities is one that utilizes a process that is robust, requires minimal chemicals and operator intervention, and produces minimal waste products (Amini et al., 2018). Two examples of these treatment processes are the granular activated carbon process and the ion exchange process.

2.4 Granular Activated Carbon (GAC), Biological Activated Carbon (BAC), and NOM Removal

Activated carbon (AC) is a common NOM removal technology for drinking water and can be described as either granular activated carbon (GAC) or powdered activated carbon (PAC), depending on the coarseness of the media. Details will be provided for GAC, as only GAC technology was used for this research.

The adsorptive capacity of GAC comes from its porous structure; these pores vary in size from below 2 nm (micropores) to above 100 nm (macropores) and in between (mesopores) (Buchanan et al, 2008; Schwanke et al., 2019; Sillanpää, 2015). The porosity of GAC has a large impact on DOC removal efficiency as the pores provide surface area for the physisorption of NOM. Another major factor impacting DOC removal from water is the empty bed contact time (EBCT), which is defined by equation (1) below:

$$EBCT = \frac{V_F}{Q} \quad (1)$$

where V_F is the volume of the media (L), Q is the flow velocity (L/min), and EBCT is the empty bed contact time (min) (Crittiden, 2012). EBCT describes the amount of time it takes for a volume of water equivalent to the volume of the media bed to travel through the bed. Increasing the flow rate results in water spending less time in contact with the removal media. For a GAC process removing DOC, the EBCT is commonly between 5 and 30 minutes (Crittiden, 2012).

GAC exhaustion occurs when the media is saturated with organics. Once GAC is exhausted, there will be negligible DOC adsorption and the GAC can either be replaced with fresh GAC or it can be left in operation to allow biofilm growth on the media. Allowing biofilm growth on the GAC media to perform DOC removal is known as biological activated carbon (BAC). The biofilm on the media actively participates in DOC removal by biodegradation. GAC media provides an excellent surface for biofilm to adhere to, and heterotrophic bacteria within this biofilm consume the biodegradable organic matter (BOM, or BDOM when dissolved, Figure 2-2) (Crittiden, 2012). The removal of BDOM reduces the formation of biofilm in subsequent processes or distribution lines. The DOC removal of BAC varies between 5% and 20% of inlet DOC concentrations depending on operating conditions and biofilm characteristics, DOC, and activated carbon (Buchanan et al., 2008; Gibert et al., 2013; Lu et al., 2020; Servais, 1995).

2.5 Ion Exchange (IEX) and NOM Removal

Ion exchange (IEX) is another NOM removal technology and can be described as either anionic or cationic, depending on the charge of the ions loaded on the resin. IEX is frequently used for water softening and demineralization whereby cations like calcium and magnesium, and anions like chloride (Cl^-), sulphate (SO_4^{2-}), and nitrate (NO_3^-) are removed from water (Crittiden, 2012). For DOC removal by anion exchange resins, exchange takes place between the negative ions loaded on the exchange resins (known as 'counter-ions') and the negatively charged DOC in the water (known as 'co-ions'), thereby removing DOC (Cornelissen et al., 2008). Resin affinity for different ions is affected by the valence and atomic number of the ions being exchanged, as well as the different functional groups present on the resin backbone at neutral pH (Crittiden, 2012). For strong-base anionic resins, the there exists an affinity trend, in order from greatest to lowest affinity: DOC > SO_4^{2-} > NO_3^- > Cl^- (Crittiden, 2012). Variations in DOC composition can affect this selectivity, as seen in the work performed by Liu et al., who saw the following affinity trend between different NOM fractions: NOM3 > SO_4^{2-} > NOM2 > NO_3^- > Cl^- and a third fraction, NOM1, was not exchanged at all (Liu et al., 2020). As seen in Figure 2-1, there are various functional groups such as carboxylic acids that become deprotonated at pH ~7, and the number of these groups in a molecule of NOM will affect the overall charge and the affinity to anionic resins. This makes IEX columns containing strong-base anionic exchange resins good candidates for the treatment of drinking water sources, with DOC removal reported as 60 – 80% (Amini et al., 2018; Winter et al., 2018). In a paper by Bolto & Dixon in 2002, the DOC removal efficiency of different resin types was explored. They found a strong correlation between the increasing water content of the resins and an increase in the percentage of UV absorbers

removed. They also found that an acrylic microporous resin generally performed better in DOC removal than gel styrene resin (Bolto & Dixon, 2002).

Following the findings of Bolto et. al. and congruent with previous works by our research collaborators, the Purolite A860 resin was chosen for this research. Purolite A860 is an acrylic, macroporous, strong-base anionic resin loaded with chloride counter-ions on its quaternary ammonium functional groups (Purolite, 2021). An example of a typical IEX resin bead is shown in Figure 2-3 below:

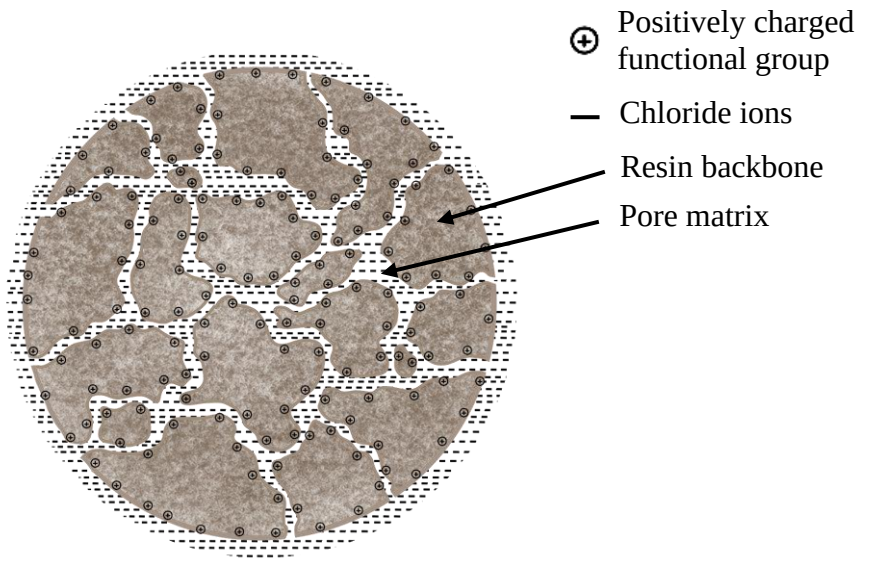

Figure 2-3: Stylized model of an anionic resin bead.

Purolite A860 is often used for drinking water treatment, with high flow rates and an EBCT between 3 and 10 minutes (Zimmermann et al, 2021). Strong-base anionic resin removal of DOC follows equation (2) below (Sillanpää, 2015):

$$Resin - NMe_3^+Cl^- + DOC^- \leftrightarrow Resin - NMe_3^+DOC^- + Cl^- \quad (2)$$

As DOC is attached to the resin, chloride is released in charge-equivalent amounts to maintain charge neutrality on the resins and in the bulk solution. This charge equivalency allows for the resin saturation to be examined, as the mass of accumulated ions is converted to milliequivalents and compared against the theoretical resin capacity given in milliequivalents. The conversion from mass to milliequivalents is shown in equation (3):

$$\frac{(X_{out} - X_{in}) * -1}{1000} * CD_X \quad (3)$$

where X is the mass of the compound of interest and CD_X is the charge density of that compound. Each compound of interest has a charge density in mEq/g associated with it, calculated based on the molar charge and molecular weight using equation (4):

$$CD_X = \frac{|Ionic\ Charge_X|}{MW_X} * 1000 \quad (4)$$

Once all chloride has been released, the DOC removal potential of the resins is reduced, and regeneration is typically performed. Regeneration of chloride-form resins is accomplished by passing a high concentration salt brine (typically NaCl) through the filter media bed to overcome the affinity preference for DOC and sulphate, which desorbs DOC and reloads the functional groups on the resin with chloride ions. Equation (5) describes regeneration: (Sillanpää, 2015):

$$Resin - NMe_3^+DOC^- + Cl^- \leftrightarrow Resin - NMe_3^+Cl^- + DOC^- \quad (5)$$

This high concentration brine is collected in a waste bin to be properly disposed of. Due to the high affinity of anion exchange resins for DOC, chloride exhaustion occurs rapidly, requiring ion exchange columns to be regenerated on a weekly basis.

2.6 Biological Ion Exchange (BIEX) and NOM Removal

The brine required for regeneration of IEX resins poses transportation and disposal issues for remote communities. Biological ion exchange (BIEX) is a technology that mitigates the challenges created by IEX regeneration. In BIEX, the regeneration step is delayed well beyond resin chloride exhaustion: once the resins are exhausted, naturally occurring biofilm is encouraged to grow on the resin media and the biological activity of the biofilm continues removing DOC from water. Flow through BIEX media is slower than for IEX operation, flowing with an EBCT of between 10 and 30 minutes versus 3-5 minutes for IEX; this increased contact time allows for additional anion exchange and removal of DOC.

To date, BIEX has been successful in removing DOC for extended periods of time without regeneration, showing promising results for rural and remote communities. The first full scale BIEX treatment plant was installed in the community of Dzit'lain'li, also known as Middle River, lifting a 14-year BWA in 2018 (WSP, 2018a). Using BIEX, the community saw an average 80% reduction in DOC over the first year of operation and allowed for effective UV and chlorine disinfection (Zimmermann, et al., 2020).

Winter et al. (2018) performed both biotic and abiotic column tests to determine how long each column would run for until breakthrough was reached, with breakthrough defined as $C/C_0 = 0.7$ or when effluent DOC concentration exceeded 2 mg/L, to examine biofilm impact on DOC removal. The DOC concentration for both waters was diluted to 5 mg/L. Breakthrough in the abiotic columns was reached after 37 days for both Suwannee River and Jericho Pond water. For the biotic columns, breakthrough was reached after 94 days for Suwannee River water and was not reached after 11 months for Jericho Pond water. This study suggested that the

characteristics of NOM had an impact on the stability of the BIEX columns, and also recognised the contribution of microbial community to DOC removal (Winter et al., 2018).

It has been well documented that sulphate ions compete for active sites on IEX resins and can inhibit removal of DOC (Ates & Incetan, 2013). BIEX remains unregenerated for much longer than IEX, and it is now thought that ion exchange occurs in two stages in BIEX: primary ion exchange, where DOC is exchanged with chloride ions, and secondary ion exchange, where DOC is exchanged with sulphate ions (Amini et al., 2018; Liu et al., 2020; Zimmermann et al, 2021). Pure biodegradation of DOC was not investigated in the aforementioned works. Amini et. al. performed a study in 2018 looking at BIEX compared to IEX, GAC, and BAC. Breakthrough (exact definition not specified) occurred after 92 days when DOC removal was ~57%, however the DOC removal increased and remained at 64% through the summer, an additional ~137 days. They found that chloride was completely exhausted from their BIEX column after 90 days, coinciding with a reduction in DOC removal. After chloride exhaustion, the DOC removal improved; it is suggested that this phenomenon may be due to displacement of other anions and biodegradation (Amini et al., 2018).

In a later study by Liu et al. in 2020, it was seen that chloride was displaced by sulphate and two fractions of NOM they called NOM2 and NOM3. After chloride exhaustion, they saw sulphate displacing NOM2, while NOM3 continued to displace sulphate. The first fraction, NOM1, did not exchange with the column at all. These observations describe the primary and secondary IEX phases, whereby sequentially chloride and then sulphate are displaced from the column, showing the importance of sulphate in the removal of DOC from water (Liu et al., 2020).

In 2021, Zimmermann et al. found that primary IEX loaded mostly sulphate to the resins, and a higher concentration of sulphate in the inlet caused less DOC to be removed from the water, suggesting that the resins had a higher affinity for sulphate than DOC. They also noted that the transition of sulphate uptake to its release coincided with the exhaustion of chloride ions. After the DOC concentration in the inlet water was increased, an increase in DOC uptake onto the resins corresponded with a release of sulphate, supporting the theory of a secondary IEX mechanism (Zimmermann et al., 2021).

Edgar & Boyer (2021) performed a comparison of regenerated and non-regenerated (BIEX) columns in 2021, aiming to explore the mechanism behind DOC removal in non-regenerated columns. These experiments were performed using upflow columns, whereas all other column tests mentioned were performed in downflow mode. The regenerated columns had better DOC removal performance than the non-regenerated columns at around 75%, and their ion release ratio (equivalents [eq]) ions removed to eq ions released) was approximately 1, indicating primary IEX. The non-regenerated columns had around 50% DOC removal, in line with previous research, and the ion release ratio was much less than unity, between 0.2 and 0.6, indicating excess ion release and secondary IEX. Biodegradation, which would have been indicated with an ion release ratio greater than units, was not seen. In plotting the percent of active sites occupied by chloride, sulphate, and DOC, Edgar & Boyer show that there was accumulation of sulphate and DOC as chloride was released from the regenerated columns. For the non-regenerated columns, there was a steady accumulation of DOC over time, as expected, and sulphate also loaded onto the resins while chloride was releasing. Once all chloride was released, the columns began to release sulphate, continuing the slow accumulation of DOC through secondary IEX. In addition to the resulting support of secondary IEX, Edgar & Boyer also performed measurements

of adenosine triphosphate (ATP), confirming the increasing presence of biological activity in the non-regenerated columns, and fluorescence excitation emission matrices (EEM's) along with low effluent specific ultraviolet absorbance (SUVA) results indicated that IEX primarily removed terrestrial DOC, in line with previous research (Edgar & Boyer, 2021).

Allowing ion exchange resins to proceed through both primary ($Cl^- \leftrightarrow DOC/SO_4^{2-}$) and secondary ($SO_4^{2-} \leftrightarrow DOC$) ion exchange mechanisms extends the operating life before regeneration is required. Additionally, encouraging the growth of biofilm is suspected to increase DOC removal through biodegradation. As mentioned in section 2.4, biodegradation in BAC is responsible for about 5-20% DOC removal, and it is suspected that a similar biodegradation of DOC occurs in BIEX. The processes of primary and secondary IEX, as well as biodegradation, reduce both the amount of brine waste produced and frequency of operator intervention.

2.7 Knowledge Gaps

Previous studies have shown that biological ion exchange (BIEX) is a potential technology for NOM removal, and is of particular interest for use in remote communities (Amini et al., 2018; WSP, 2018b; Zimmermann et al., 2021). Not yet explored is how a high level of DOC in the source water can impact the removal efficiency of BIEX, as previous studies have not seen inlet DOC levels exceed 8 mg/L, as shown in Table 2-1. It is important to note that, as secondary IEX is further explored and understood, the concentration of DOC is not the only factor impacting DOC removal from water; ions in the water, particularly sulphate, also play a role.

Table 2-1: Source Water Characteristics for Related BIEX Studies

DOC Concentration (mg/L)	Sulphate Concentration (mg/L)	Study
7.09 ± 0.34	6 – 10	(Amini et al., 2018)
2.5 ± 0.2	28.2 ± 4.5	(Liu et al., 2020)
4.79 (batch 1)	61.4	(Edgar & Boyer, 2021)
4.96 (batch 2)	45.7	
2.9 ± 0.2 (period 1)	63.1 ± 3.3 (high sulphate)	(Zimmermann et al., 2021)
5.1 ± 0.3 (period 2)	11.5 ± 1.3 (low sulphate)	

One knowledge gap to be addressed in this work therefore is:

- What is the performance of BIEX in long-term field operation treating raw water with a high inlet DOC concentration of 8 – 10 mg/L?

BAC has shown maximal DOC removal of 5 – 20% due to biodegradation, and BIEX has so far seen DOC removal greater than 30% (Amini et al., 2018; Edgar & Boyer, 2021; Liu et al., 2020; Zimmermann et al., 2021). As it is suspected that the extent of biodegradation in BIEX would be similar to the biodegradation seen in BAC, complete resin exhaustion may not have yet been observed. One such example of this is in the paper by Edgar & Boyer, seen in Figure 2-4 below, showing that secondary IEX was not yet complete as sulphate was still releasing.

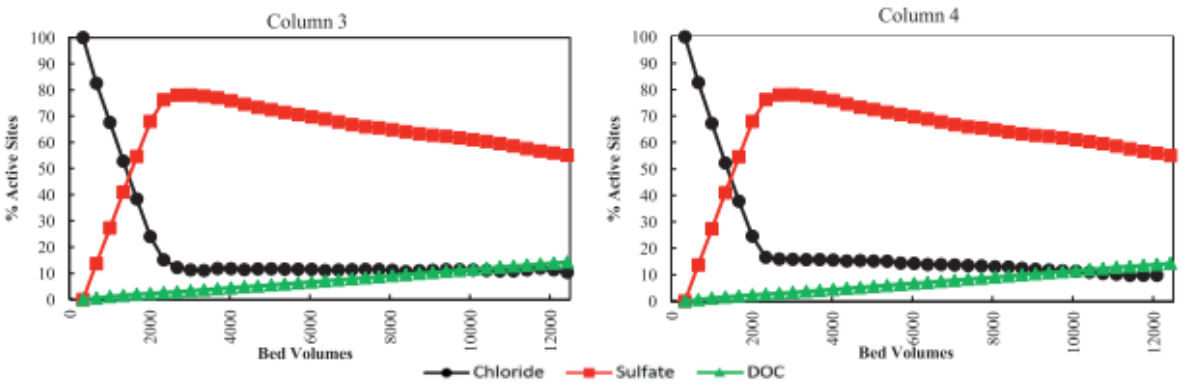

Figure 2-4: Percentage of active sites occupied by chloride, sulfate, or DOC in the 2021 paper written by Edgar & Boyer, showing the transition of the resins from primary IEX to secondary IEX. Also seen is the over 50% sites still containing sulphate, suggesting secondary IEX had not yet finished. Adapted from Edgar & Boyer, 2021.

As GAC exhaustion occurs when all adsorption sites are occupied, and it is yet unknown that any additional mechanisms aside from biological removal occurs in BAC, it may be assumed that the base removal of DOC due to biological activity should be around 5 – 20% as noted in the paper by Roberts & Summers (1982), leading to the question of whether BIEX resins have been completely exhausted in previous studies (Roberts & Summers, 1982). This leads to additional knowledge gaps:

- Is there a point at which all sulphate is released, and what is the performance of BIEX in this state?
- Is this state biodegradation or a tertiary IEX?

Finally, as there may have not been full exhaustion of BIEX resins, the final knowledge gap is:

- Is there a capacity change of regenerated BIEX resins after complete exhaustion due to DOC adsorption in field operation?

Chapter 3: Research Approach and Objectives

3.1 Research Approach

As discussed in Chapter 2:, BIEX is a promising technology for rural communities. The quality of the water in each community, along with remoteness, impacts the technologies that can be useful for potable water treatment. The community of Gillies Bay Improvement District (GBID) is a rural community whose drinking water source has high DOC (9.1 ± 0.1 mg/L) and low sulphate (2.9 ± 0.1 mg/L), nitrate (~ 0.7 mg/L), and chloride (~5 mg/L) ions. In the summer, GBID deals with drinking water advisories due to high coliforms and insufficient treatment. To examine the efficacy of treatment options for this community and technologies in treating high DOC content water, RESEAU Centre for Mobilizing Innovation (RESEAU CMI) and its partners transported a mobile laboratory to the community of GBID. The mobile laboratory was equipped to pilot four different technologies: ion exchange (IEX), biological ion exchange (BIEX), granular activated carbon (GAC), and biological activated carbon (BAC). This pilot project remained on site and operational in GBID for 18 months (April 2020 to October 2021) to determine the performance of each technology as they are impacted by seasonal water changes. Sampling was performed thrice weekly by the local water operator and monthly site visits were undertaken for detailed analysis, experiments, and maintenance.

This pilot project was accompanied by a UBC laboratory component, whereby IEX resin samples were extracted monthly from the pilot column and shipped to UBC. These laboratory experiments examined the impact of DOC accumulation on the ion exchange resins. Regeneration experiments performed examined the resin capacity before and after regeneration, and the differences between on-site and in-laboratory resin regeneration. The results of the pilot

and laboratory experiments will be used to advise the community as they work towards developing a full-scale treatment system.

3.2 Research Objective and Hypotheses

The main objective of this work was to determine the efficacy of (BIEX) in treating high organics water as addressed in the following hypothesis:

- Water with an average DOC concentration of 9 mg/L can be treated by biological ion exchange to achieve > 50% removal of DOC without regeneration for 9 months.

Samples were collected thrice weekly from GBID and shipped to the University of British Columbia (UBC) to measure the ultraviolet absorbance at 254 nm (UVA_{254}), DOC concentration, and various ion concentrations. These data allow for the DOC removal to be compared against trends in adsorption and release of ions from the IEX resins, yielding insights into the mechanisms behind primary IEX, secondary IEX, and biodegradation. Additionally, the data from this first objective will help the community of GBID on their quest for clean water.

A secondary objective of this work was to determine how full resin exhaustion affects the capacity of Purolite A860, the strong-base anionic exchange resin used in this study. This can be summarized with the following hypothesis:

- Accumulation of dissolved organic carbon on Purolite A860 to full resin exhaustion reduces the overall resin capacity of the resin after regeneration.

To explore this hypothesis, monthly resin samples were removed from the ion exchange column and shipped to UBC. An aliquot of these resins was subject to multiple loading tests

(MLTs) to determine their remaining capacity. Resins were also extracted before and after on-site regeneration to examine regeneration efficacy between on-site and in-lab regenerations.

Chapter 4: Experimental Methodology and Procedures

Two separate sections are used to describe the methodologies and procedures used in the 1) pilot scale (GBID pilot study) and 2) laboratory scale studies.

4.1 Reagents and Chemicals

4.1.1 Anionic Exchange Resin

Previous studies have shown that Purolite A860 strong base anionic exchange resin is promising in the removal of natural organic matter (NOM) from drinking water (Amini et al., 2018; Brezinski et al., 2019; Liu et al., 2020; Schulz et al., 2017; Winter et al., 2018; Zimmermann et al., 2021). Hence, the A860 resin was chosen for this long-term study. The properties of this resin are outlined in Table 4-1.

Table 4-1: Characteristics of Purolite A860 Anion Exchange Resin

Characteristic	**Value***
Polymer structure	Macroporous polyacrylic crosslinked with divinylbenzene
Appearance	Spherical beads
Functional group	Quaternary ammonium
Ionic form	Chloride form
Total capacity (minimum)	0.8 Eq/L resin
Particle size range	300 – 1200 µm
Specific gravity	1.08

* Values provided by the manufacturer (Purolite, 2021)

4.1.2 Activated Carbon

To compare the DOC removal efficiency of Purolite A860 ion exchange resin against commonly used technology, AlamoBrand granular activated carbon (GAC) was used. The characteristics of this GAC are outlined in Table 4-2.

Table 4-2: Characteristics of AlamoBrand Activated Carbon

Characteristic	**Value**
Media Type	Coconut shell carbon
Particle Size	12 x 40 mesh
	0.425 – 1.70 mm

4.1.3 Reagents

Laboratory regenerant solutions were prepared using sodium chloride (NaCl, ThermoFisher CAS 7647-14-5, Waltham, MA) and deionized water (resistivity of 18.2 M.Ω.cm). Field regenerant solutions were prepared using NaCl in the form of water softener salt from a local hardware store (Windsor Salt, Pointe-Claire, QC) and untreated water from the nearby Cranby Lake.

4.2 Glassware

All glassware were soaked in mild acid (0.1 wt.% HCl) overnight, before being rinsed three times each with tap and deionized water. Glass was then wrapped in aluminium foil and baked in a Lindberg/Blue M Box furnace (ThermoFisher Scientific, Waltham, MA) at 550 °C.

4.3 Analytical Techniques and Procedures

4.3.1 Physical Water Characteristics

Turbidity, pH, and temperature were all measured and recorded by the local water operator at time of sampling using equipment shown in Table 4-3.

Table 4-3: Field Equipment for Physical Water Characteristic Measurements

Parameter	**Instrument**
Turbidity	HACH 2100P portable turbidimeter
pH + Temperature	HANNA pHep5 portable waterproof pH and temperature tester

4.3.2 Dissolved Organic Carbon (DOC)

Dissolved organic carbon (DOC) was measured using a GE Sievers M5310C TOC analyzer (Suez, La Défense, Paris), using the persulfate-ultraviolet method, Standard Method 5310C (Baird et al., 2017). Deionized (DI) water blanks and standard solutions with known 5 and 10 mg/L concentrations were analysed at the start and end of each sequence and all sample TOC values were corrected to this standard. The detection limit of the GE TOC analyser is around 0.2 mg/L. Samples were filtered using 0.45µm polyvinylidene difluoride (PVDF) syringe filters (Merck Millipore Ltd., Carrigtwohill, Co. Cork) to eliminate particulate (Baird et al., 2017). Samples were filtered directly into 40 mL amber glass vials, covered in aluminium foil, and loaded into the instrument trays. An autosampler introduced 10 mL of sample through three injections into the instrument, which injected 6 M phosphoric acid (H_3PO_4) to the sample to drop the pH to 2 for more accurate total carbon (TC) and inorganic carbon (IC) measurements. 15% ammonium persulphate [$(NH_4)_2S_2O_8$] was added to the sample to oxidize organics and inorganics, before splitting the sample into two equal but separate streams for measuring TC and

IC. The TC stream was passed to an oxidation reactor, where the sample was exposed to UV light at both 185 nm and 254 nm, which produced hydroxyl radicals to oxidize the organics in the sample into carbon dioxide (CO_2), as per equations (6), (7), (8), and (9) (Suez, 2017):

$$H_2O + hv\ (185nm) \rightarrow OH\cdot + H\cdot \quad (6)$$

$$S_2O_8^{-2} + hv\ (254nm) \rightarrow 2\ SO_4^-\cdot \quad (7)$$

$$SO_4^-\cdot + H_2O \rightarrow SO_4^- + OH\cdot \quad (8)$$

$$Organic\ Compounds + OH\cdot \rightarrow CO_2 + H_2O \quad (9)$$

The IC stream passes through a delay coil to make analysis time for TC and IC the same. After the TC stream exited the reactor and the IC stream exited the delay coil, the streams were then passed through separate membranes, which allowed only CO_2 to pass through while any by-products or contaminants remained on the sample side. The resulting CO_2 from each stream was sent to separate conductivity cells that measured the amount of CO_2 produced from the sample by analyzing the difference in conductivity between high purity DI water and the DI water containing the dissolved CO_2, and this change was converted into an amount of IC or TC. The total organic carbon (TOC) was then calculated using equation (10):

$$TOC = TC - IC \quad (10)$$

The CO_2 that passed through the membrane entered a closed DI water loop. The CO_2 reacted with water to produce hydrogen and bicarbonate (HCO_3^-) , as per equation (11):

$$CO_2 + H_2O \leftrightarrow H_2CO_3 \leftrightarrow H^+ + HCO_3^- \quad (11)$$

The ion exchange resin bed removed the HCO_3^- and other ions in the DI, keeping the DI stream clean and free from contaminants. Error was determined using standard deviation of results from three injections.

4.3.3 Inorganics Composition

4.3.3.1 Anion Concentration

Concentrations of other ions present in the water, including chloride, nitrate, and sulphate were measured according to the standard method 4110B (Baird et al., 2017) using a Dionex ICS-1100 ion chromatograph (Waltham, MA). The instrument injected the sample into an eluent stream, composed of sodium carbonate and sodium bicarbonate concentrate ($NaHCO_3$ and Na_2CO_3) (Dionex AS22 eluent concentrate, ThermoFisher Scientific, Waltham, MA), which helps to separate the ions in the sample. This sample was passed through a guard column to remove contaminants and was sent to an analytical column (AS22-Fast column), which separated the ions via ion exchange. The ions move through the column at different rates depending on the interaction of the ions with ion exchange sites. The sample then traveled to a suppressor, which enhanced the detection of the ions and supressed eluent conductivity, before moving to a conductivity cell. The cell measured the conductivity of the sample ions as they exited the suppressor. Each ion was identified based on the retention time inside the system, while the concentration was determined by Chromelon software performing an integration of the signal peaks produced. Prior to analysis, each sample was filtered with 0.45µm PVDF syringe filters (Merck Millipore Ltd., Carrigtwohill, Co. Cork) and 5 mL of filtered sample was used to fill the IC PolyVials (ThermoFisher Scientific, Waltham, MA), which were placed into the autosampler. The instrument analysed each sample twice, and an average of these values was reported. Blanks of deionized water and standard, prepared using 10 times diluted Dionex seven anion standard II (ThermoFisher Scientific, Waltham, MA), were measured at the beginning and end of each sequence to confirm accuracy of the instrument, and each sampled value was corrected to these standards. Error was determined using standard deviation of results.

4.3.3.2 Alkalinity

The alkalinity of each sample was measured with a HANNA HI83303 aquaculture photometer (Woonsocket, RI). The photometer used a colorimetric method to determine the amount of alkalinity in the sample (US EPA, 1974). 10 mL of sample was added to a cuvette and used to blank the instrument. 1 mL of alkalinity reagent (HI776-26) (HANNA Instruments, Woonsocket, RI) was added to the sample, mixed gently, and placed in the instrument for reading; the alkalinity measurement is returned as mg/L $CaCO_3$. The range of the instrument was 0 – 500 mg/L as $CaCO_3$ and the error was 5 mg/L ± 5% of reading.

4.3.4 UV Absorbance at 254nm (UVA_{254})

The ultraviolet absorbance at 254nm (UVA254) was measured using a Cary 100 UV-Vis spectrophotometer (Agilent Technologies, Santa Clara, CA) according to the ultraviolet absorption method 5910 B (Baird et al., 2017). A clean quartz cuvette with a path length of 1 cm was filled with deionized (DI) water and used to blank the instrument, set to detect at 254 nm. After blanking, the DI water was discarded and replaced with sample, and the sample was measured at 254 nm. Error was determined using standard deviation of results.

4.3.5 Resin Mass

The mass of resins was required for multiple loading test (MLT) experiments, and was measured using a Shimadzu ATX224 analytical balance (Shimadzu, Kyoto, Japan), with a range up to 220 g, a 0.2 mg linearity error, and a repeatability standard deviation of ≤ 0.1 mg.

4.3.6 Statistical Analysis

All graphical error bars represent the standard deviation of analytical results of pilot scale and laboratory studies unless otherwise specified. Errors specified in the text were standard deviations of values unless otherwise explained. Some data points are presented without associated errors due to missing instrumental reports. A 95% confidence interval was also calculated during analysis, using a paired t-test for assessing the difference of two averages. Normal distribution was assumed, and the confidence interval calculated using equation (12):

$$(\overline{y_a} - \overline{y_b}) \pm t_{0.95,n-1} \times s_{\overline{y_a}-\overline{y_b}} \tag{12}$$

Where $(\overline{y_a} - \overline{y_b})$ is the difference of averages between a and b, the t-value is based on a 95% confidence interval based on a two-tailed distribution, and $s_{\overline{y_a}-\overline{y_b}}$ is the standard error.

In the cases where variance was not of the same magnitude, an Aspen-Welch t-test was performed based on the degrees of freedom (equation (13)), the standard error (equation (14)), and the calculated test statistic (equation (15)):

$$df = \frac{\left(\frac{s_a^2}{n_a} + \frac{s_b^2}{n_b}\right)^2}{\left(\frac{1}{n_a - 1}\right)\left(\frac{s_a^2}{n_a}\right)^2 + \left(\frac{1}{n_b - 1}\right)\left(\frac{s_b^2}{n_b}\right)^2} \tag{13}$$

$$SE(\overline{y_a} - \overline{y_b}) = \sqrt{\frac{s_a^2}{n_a} + \frac{s_b^2}{n_b}} \tag{14}$$

$$t = \frac{(\overline{y_a} - \overline{y_b})}{SE(\overline{y_a} - \overline{y_b})} \tag{15}$$

Where s^2 is the variance and n is the sample number. Analysis of variance (ANOVA) was also used. The method used is specified in the discussion.

4.4 Pilot Study Experimental Processes

4.4.1 Location and Source Water Characteristics

The pilot experiment took place in the community of Gillies Bay Improvement District (GBID), which is approximately 200 km by road and ferry north from the University of British Columbia (UBC, Vancouver, Canada). The location of GBID relative to UBC is shown in Figure 4-1.

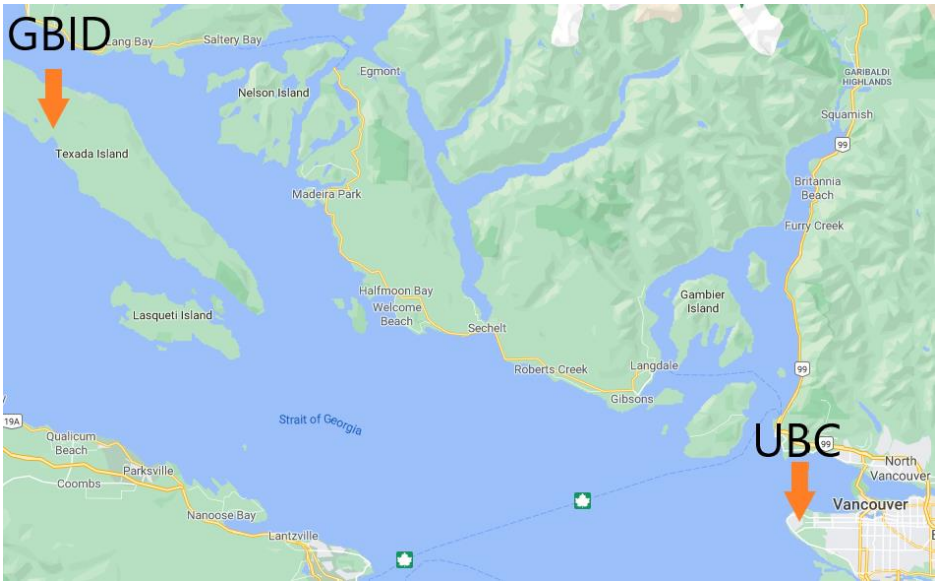

Figure 4-1: Map of British Columbia, Canada, showing the Sunshine Coast, UBC, Texada Island and Gillies Bay Improvement District (GBID).

The community has a population of roughly 500 people and the surface drinking water source is Cranby Lake, seen in Figure 4-2 (Kerr Wood Leidal, 2016).

Figure 4-2: Cranby Lake, in Gillies Bay Improvement District, BC, is the drinking water source for the community.

As a surface source, the lake is visited by animals, like birds and deer, and has unique water quality characteristics that must be examined for treatment, outlined in Table 4-4.

Table 4-4: Average Source Water Characteristics for Cranby Lake

Parameter	**Value**
Dissolved organic carbon (DOC)	9.1 ± 0.1 mg/L
Turbidity	0.5 – 1.5 ± 0.03 NTU
Ultraviolet absorbance at 254nm (UVA_{254})	0.184 ± 0.001 cm^{-1}
Alkalinity (as $CaCO_3$)	44 ± 7.2 mg/L
Sulphate	2.9 ± 0.1 mg/L

Currently, the lake water flows through a Johnson screen and is treated with chlorine before being distributed to the community. The chlorination station is shown in Figure 4-3.

Figure 4-3: Chlorination station in Gillies Bay Improvement District.

4.4.2 Experimental Setup

The pilot setup consisted of a 42 ft long towable trailer outfitted with: an inlet 60 Hz centrifugal pump (Goulds, Seneca Falls, NY); a strainer with 5 mm pores (Hayward Flow Control, Clemmons, NC); a bag filter vessel (Hayward Flow Control, Clemmons, NC) outfitted with 25 µm bag filters (Hayward Flow Control, Clemmons, NC); two cartridge filter vessels (Pentair, Minneapolis, MN) outfitted with 5 µm filter cartridges (Harmsco, Riviera Beach, FL); and two treatment columns containing ion exchange (IEX) media and granular activated carbon (GAC) media (see sections 4.1.1 and 4.1.2 respectively). The mobile laboratory was installed at the GBID test location on April 28th, 2020. Raw water flowed from Cranby Lake through the Johnson screen and into the mobile lab, where it passed through the strainer, bag filter, cartridge filter, and then split to feed the GAC and IEX columns. The process flow diagram (PFD) is shown in Figure 4-4.

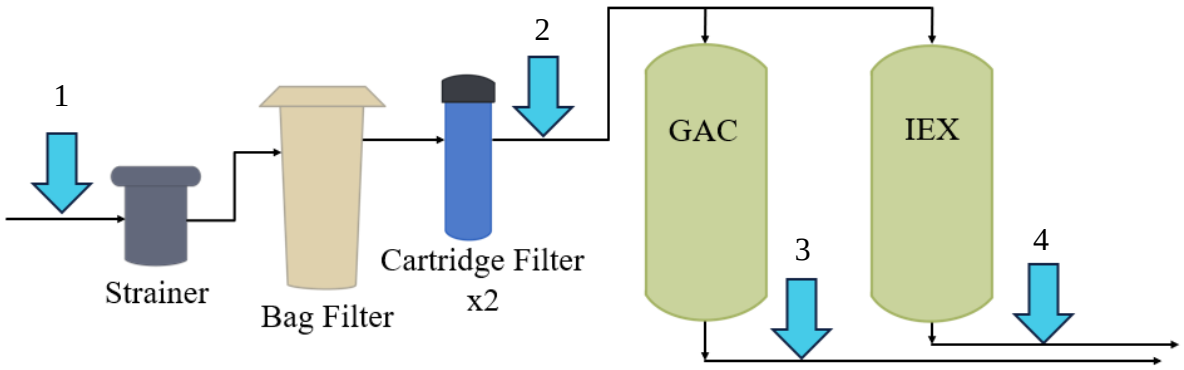

Figure 4-4: Process flow diagram for the mobile laboratory on site in Gillies Bay Improvement District, showing filters, columns, and sample locations indicated by arrows.

Water samples were collected thrice weekly from: 1) the system inlet; 2) after the cartridge filters; 3) after the GAC column; and 4) after the IEX column. All samples were shipped weekly to UBC by Canada Post, in a cooler, and arrived after approximately 2-3 days.

4.4.3 Operational Conditions

4.4.3.1 Granular Activated Carbon and Biological Activated Carbon

The activated carbon column was operated from May 25th, 2020, to October 5th, 2021. The column was opaque fibreglass, 167 cm tall and contained approximately 80 L of AlamoBrand GAC. The column was controlled by a Fusion^{2} column control head (Waterite Technologies, Winnipeg, MB, Canada) until installation of a 1" globe valve on September 8th, 2020. From September 8th, 2020, until February 17$_{th}$, 2021, the flow rate was controlled by the globe valve and monitored with a magnetic-inductive flow meter (ifm electronic, Essen, Germany), with operating conditions outlined in Table 4-5.

Table 4-5: EBCT Test Conditions for GAC and BAC

Dates	EBCT (min)	Flow Rate (L/min)	Flow Control Method
May 25th, 2020 – Sept 8th, 2020	26	3.1	Column head plug valve
Sept 8th, 2020 – Aug 31st, 2021			1" globe valve

4.4.3.2 Ion Exchange and Biological Ion Exchange

The ion exchange (IEX) and biological ion exchange (BIEX) column operated from May 27th, 2020, to October 5th, 2021. The column was an opaque fibreglass column 167 cm tall, approximately half full of 68 L of Purolite A860 resin. The column was controlled by a Fusion^2 column control head (Waterite Technologies, Winnipeg, Canada), and operated in three phases, outlined below.

4.4.3.2.1 Phase One: Variant Flow Rates

Phase one operated from May 27th to June 6th, 2020, and examined empty bed contact time (EBCT) step changes by altering flow rate. The EBCTs tested were between 1.74 min (corresponding to 39.4 L/min) and 8 min (corresponding to 8.57 L/min), outlined in Table 4-6. All flow rates were controlled by the Fusion^2 column head plug valves for these tests.

Table 4-6: Test Conditions for IEX Phase One, with Flow Rates Controlled by Column Head Plug Valve

EBCT (min)	Date(s) of Test	Flow Rate (L/min)
3	May 27th – May 29th, 2020	22.8
4	June 1st – June 4th, 2020	17.1
7	June 5th, 2020	9.79
3	June 5th, 2020	22.8
8	June 5th, 2020	8.57
5	June 5th, 2020	13.7
1.74	June 6th, 2020	39.4
6	June 6th, 2020	11.4

4.4.3.2.2 Phase Two: High Flow Rate

Phase two operated from June 23rd, 2020, to February 17th, 2021, and examined how IEX/BIEX performed under a high flow rate condition, outlined in Table 4-7. The flow rate was initially controlled by the Fusion^2 column control head valves until September 8th, when a 1" globe valve was installed upstream of the column. From September 8th, 2020, until February 17th, 2021, the flow rate was controlled by the globe valve and monitored with a magnetic-inductive flow meter (ifm electronic, Essen, Germany).

Table 4-7: Test Conditions for IEX and BIEX Phase Two

Dates	EBCT (min)	Flow Rate (L/min)	Flow Control Method
June 23rd, 2020 – Sept 8th, 2020	10	6.85	Column head plug valve
Sep 8th, 2020 – Feb 17th, 2021			1" globe valve

4.4.3.2.3 Phase Three: Low Flow Rate

Phase three ran from February 17th to October 5th, 2021, and examined BIEX performance at a low flow rate condition, outlined in Table 4-8. The flow rate was controlled by a 1" globe valve and monitored using a magnetic-inductive flow meter (ifm electronic, Essen, Germany).

Table 4-8: Test Conditions for IEX and BIEX Phase Three

Dates	EBCT (min)	Flow Rate (L/min)	Flow Control Method
Feb 17th, 2021 – Aug 31st, 2021	20	3.43	1" globe valve

4.4.3.3 Backwash

Backwash is an integral part of column operation. Backwash avoids column clogging, reduces media channelling, and removes excess biofilm and particulate matter. To perform backwash on site, water was sent through the column in a counter-current upflow direction, at a flow rate which fluidized the media inside the column to at least 50% bed expansion. This flow rate was maintained for 30 minutes. A co-current downflow rinse was then performed for 10 minutes to rinse out remaining particulate matter or biofilm, and all effluent water was sent to the waste. Backwash was performed on the same day each week for both the BIEX column and the BAC column and was controlled through the Fusion^2 column control head (Waterite Technologies, Winnipeg, Canada**)**, with a flow rate of approximately 14 L/min. Expansion started at minimum 100%; however, over months with exhaustion of the media and biofilm buildup, expansion was seen to fall to approximately 10% using the same flow rate and pressure. In February 2021, air was added during the BIEX backwash procedure as follows: approximately 30 L of water was siphoned out of the column to allow room for media bubbling, and an air compressor (Mastercraft, 125 PSI) was connected to the column using 3/8" flexible tubing. Air

was introduced in backwash flow direction for 20 minutes, allowing the media to expand and bubble vigorously, thoroughly disrupting biofilm, particulate accumulation, and any resin aggregates formed during operation. Water backwash was performed after air scouring, and bed expansion was consistently higher than water backwashes at 80 - 100%.

4.4.3.4 Regeneration

Regeneration is an important maintenance step for the operation of an IEX column and is the final step in BIEX column operation. Regeneration uses a high concentration salt brine solution (at least 10 w/v% NaCl) that flows co-current in the IEX column. This high salt concentration in the solution overcomes the resin affinity for DOC, allowing chloride ions to be adsorbed by the resins, releasing DOC from adsorption sites.

To perform regeneration on site, water softener salt (Windsor, Pointe-Claire, QC) was added to a 165 L brine tank and combined with raw, unfiltered, and unchlorinated water to the overflow line. This was stirred and left to dissolve until the hygrometer (TEKCOPLUS) read >10%, as indicated by an out-of-range symbol (E03). The tank was connected by flexible tubing to the column head, and brine was pulled into the column by way of a vacuum: water flowing into the column passed the brine hose attachment, and this created a suction to pull brine at 0.6 L/min into the column. This co-current combined flow of raw water and brine, at 2 L/min, was maintained for 60 minutes at a time, after which regeneration was stopped. The IEX resins soaked in the brine solution while the brine tank was refilled if required. This process was repeated until regeneration was complete, signified by:

- The colour of the effluent progressed through clear, to a very dark brown, and back to clarity (as seen in Figure 4-5)
- The salt concentration of the effluent progressed from negligible (an indicator of adsorption) to the same concentration as the influent salt concentration
- The turbidity of the effluent decreased to around or below 1 NTU

Brine effluent was discharged into a plastic tank on site, where it was stored for disposal.

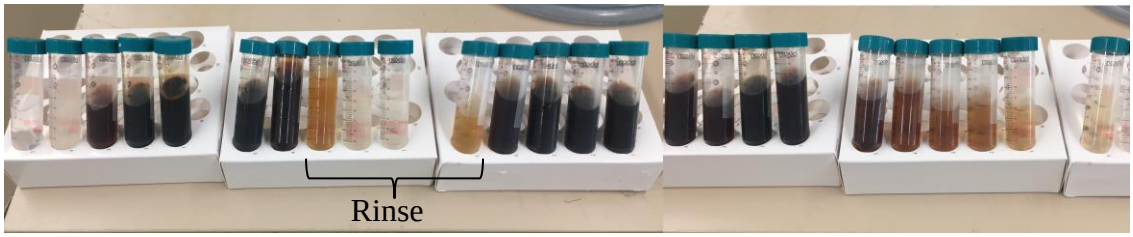

Figure 4-5: Regeneration effluent samples showing evolution of colour over six hours of regeneration on August 11th, 2021. Light samples seen in the middle of regeneration were due to a rinse performed after the first hour of regeneration.

4.5 Laboratory Study Experimental Processes

4.5.1 Source Water Characteristics

Water for the laboratory scale multiple loading test (MLT) experiments was collected from GBID on June 16th and August 12th, 2021, in 20 L containers. These containers were transported back to Vancouver and stored at 4 °C until use. Prior to use, water jugs were moved from the refrigerator to the laboratory and allowed to come to room temperature overnight. The average characteristics of the source water are outlined in Table 4-9.

Table 4-9: Characteristics of Raw Water from GBID used for Multiple Loading Tests.

Parameter	Value
Dissolved organic carbon (DOC)	9.0 ± 0.1 mg/L
UVA_{254}	0.176 ± 0.001 cm^{-1}
Alkalinity (as $CaCO_3$)	46 ± 7 mg/L
Sulphate	2.67 ± 0.22 mg/L

4.5.2 Experimental Setup

The laboratory setup for the multiple loading tests (MLTs) consisted of a Phipps and Bird PB-900 Series jar tester (Phipps & Bird, Richmond, VA), four 1 L glass beakers, Purolite A860 resin, a vacuum pump with glass filtering apparatus, and 0.45 µm paper filters. Resins used for MLTs were extracted from the BIEX column on June 6th, 2020; September 10th, 2020; February 16th, and February 17th, 2021, before and after regeneration, respectively. Pristine Purolite A860 was also used. Resins were stored in 50 mL falcon tubes at 4 °C.

4.5.3 Operational Conditions

4.5.3.1 Resin Weights

1 mL of each month's resins was measured by weight. A vacuum pump was connected to a 1000 mL filtering flask and a glass base, and a 0.45 µm paper filter (Merck Millipore Ltd., Carrigtwohill, Co. Cork) was placed on the base. Using a metal scoop, resins were transferred to the paper filter and the glass funnel was clamped to the base. DI water was used to rinse the resins, vacuum was applied, and the resins were left to dry for 4 minutes. After vacuum drying, resins were transferred to a weigh boat and weighed using an analytical balance (Shimadzu ATX224, Kyoto, Japan). 3 mL of DI water was added to a 10 mL glass graduated cylinder and the vacuum dried resins were added to the graduated cylinder until it read 4 mL. The weigh boat,

less 1 mL of resins, was weighed again and recorded. This was repeated three times for each resin sample.

4.5.3.2 Experimental Procedure

One day before the MLTs, the 20 L GBID raw water jug was moved into the laboratory to warm up to room temperature and help control for temperature effects.

Using the method outlined in section 4.5.3.1, 1 mL of resin was added to a clean, dry 1000 mL glass beaker. Using a 500 mL graduated cylinder, 1000 mL of raw, unfiltered GBID water was added to the beaker, then placed into the jar tester, seen in Figure 4-6.

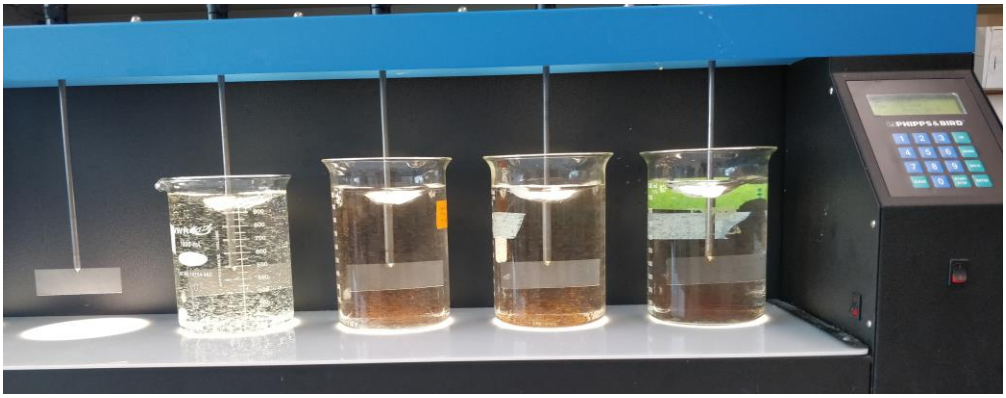

Figure 4-6: Phipps & Bird jar tester stirring four MLT beakers containing resin and raw GBID water.

This was mixed at 150 RPM and afterwards the water was separated from the resin using the same vacuum pump apparatus. Another 1000 mL of raw, unfiltered GBID water was added to the resin in the beaker. These tests were run for 17 and 43 minutes (283 and 717 bed volume [BV]) to help remove any particulate matter clinging to the resin from storage in BIEX column water. Regular tests were run for 60 minutes, corresponding to 1000 BV for each test. During separation of water and resin, 100 mL of treated water was collected for analysis of DOC,

UVA_{254}, anion concentration, and alkalinity. At the end of each day when MLTs were performed, analysis was completed on the samples from that same day.

4.5.4 Regeneration

Regeneration was performed in the laboratory on the February 16th, 2021, resin sample. Solid NaOH (Fisher Scientific, Hampton, NH) was mixed into deionized water at 10% w/v as the regeneration brine solution. 110 mL of brine solution was added to 1 mL of resins, placed into the jar tester, and mixed at 150 RPM for 60 minutes. Resins were separated from spent brine before fresh brine was introduced. This was performed three times, with no rinse in between, for a total of three 1-hour regenerations with fresh brine. Following regeneration, the resins were rinsed 10 times with DI water, with each rinse lasting 5 minutes. Fresh Purolite A860 resins were regenerated once, for one 1-hour in 10% w/v salt brine, and the setup is shown in Figure 4-7.

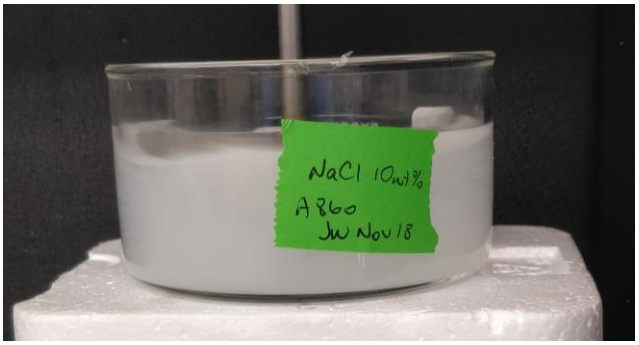

Figure 4-7: Laboratory regeneration setup showing ongoing regeneration of fresh Purolite A860 resins.

Chapter 5: Pilot Study Results and Discussion

5.1 Granular Activated Carbon (GAC) / Biological Activated Carbon (BAC)

The GAC/BAC column was run to determine the DOC removal efficiency for GBID water, and to compare the efficiency of IEX and BIEX against.

5.1.1 Dissolved Organic Carbon (DOC) Removal

Figure 5-1 shows the DOC removal and the influent water temperature for the activated carbon column. The column operated from May 25th, 2020, to October 5th, 2021, approximately 466 days in operation or 24,000 BV. During the first two days of operation, the column operated at a 10 min EBCT, corresponding to 144 BV/day. During these two days, there was an issue with column head operation causing raw influent to mix with the treated effluent, and this issue was resolved by June 4th, 2020. On June 23rd, the column went into continuous operation at an EBCT of 26 minutes, corresponding to approximately 55 BV/day, until October 5th, 2021.

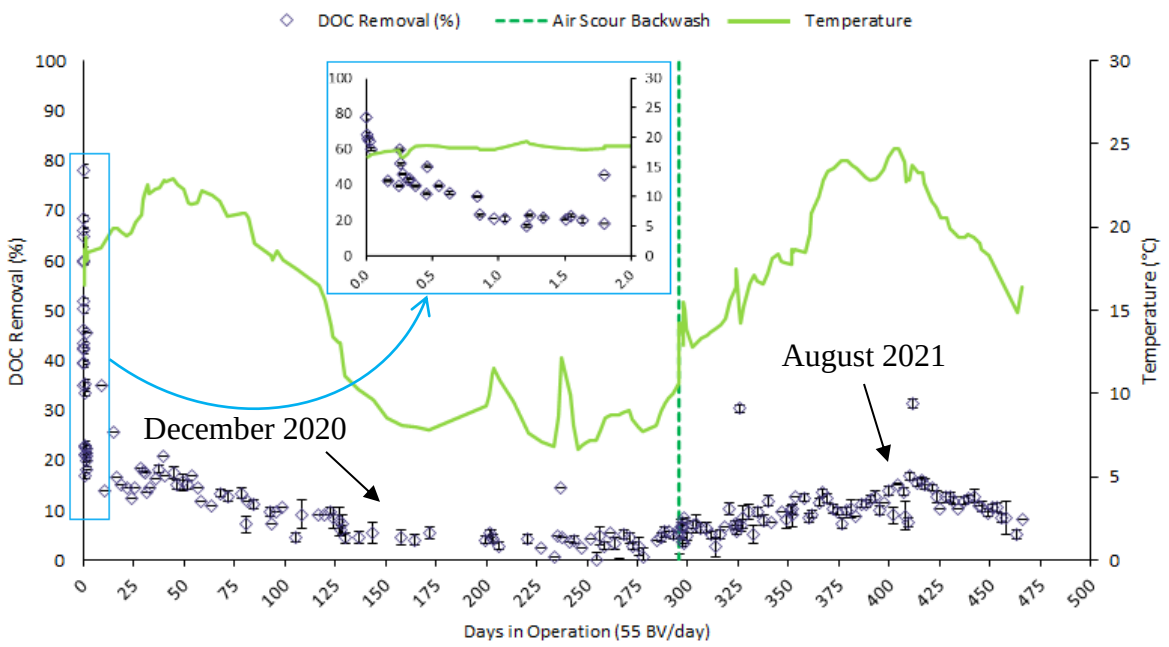

Figure 5-1: DOC removal in percentage for the GAC column, shown with the source water temperature, over the 466 days the column was in operation.

The influent DOC concentration ranged between 6.6 ± 0.1 mg/L and 14.8 ± 0.2 mg/L, averaging 9.1 ± 0.1 mg/L. The maximum DOC removal of 78 ± 1.3% occurred at the beginning of the experiment, on May 25th, and continuously decreased over 43 hours (260 BV at the end of June 4th, 2020) when the final DOC removal average was 20.2 ± 0.7%. The average DOC removal during the first 8000 BV was 23.1 ± 0.6%, lower than what was seen in the pilot study in Laval; however, their influent water was pretreated by conventional water treatment methods and ozonation, which increased the biodegradable DOC (BDOC) (Liu et al., 2020). Low DOC removal was expected, as the DOC removal method was suspected to have transitioned from adsorption to biodegradation by 200 BV, indicated by the DOC removal of approximately 20% (Emelko et al, 2006; Liu et al., 2020; Winter et al., 2018). As expected, the DOC removal of BAC was affected by temperature: bioactivity has been shown to increase in warmer temperatures (Bellamy et al, 1985; Liu et al, 2022; Mozalski et al, 1999). Figure 5-1 shows that

the DOC removal dropped, averaging 3.2 ± 0.8% between 130 and 290 days (November to April) and rose between 310 and 430 days (May to September), averaging 10.7 ± 0.9%.

On day 296 (April 16th, 2021) an air scour backwash took place which showed no significant effect on the removal of DOC, agreeing with the findings of Emelko et al. (Emelko et al., 2006). The air scour backwash may not have affected the occupied adsorption sites or biofilm and therefore had little effect on the DOC loading or biodegradation rate. Regular backwashes (water only) occurred weekly and did not have any significant effect on DOC removal.

5.1.1.1 UV Absorbance at 254 nm (UVA_{254})

Figure 5-2 shows the influent and effluent UVA_{254} of the GAC column over the first two days of operation, when the column was operated at a 10 min EBCT. The effluent UVA_{254} increased from 0.021 ± 0.002 cm^{-1} at the start of operation to 0.145 ± 0.002 cm^{-1} at the end of the first two days and agreed with results seen in section 5.1.1. During this time, there was a significant difference between the influent and effluent values, indicating ongoing removal of UV–absorbing materials. The roughly logarithmic trend is indicative of the adsorption sites steadily becoming either occupied by UV-absorbing materials or rendered inaccessible due to biofilm coverage, increasing the UV-absorbing materials in the effluent.

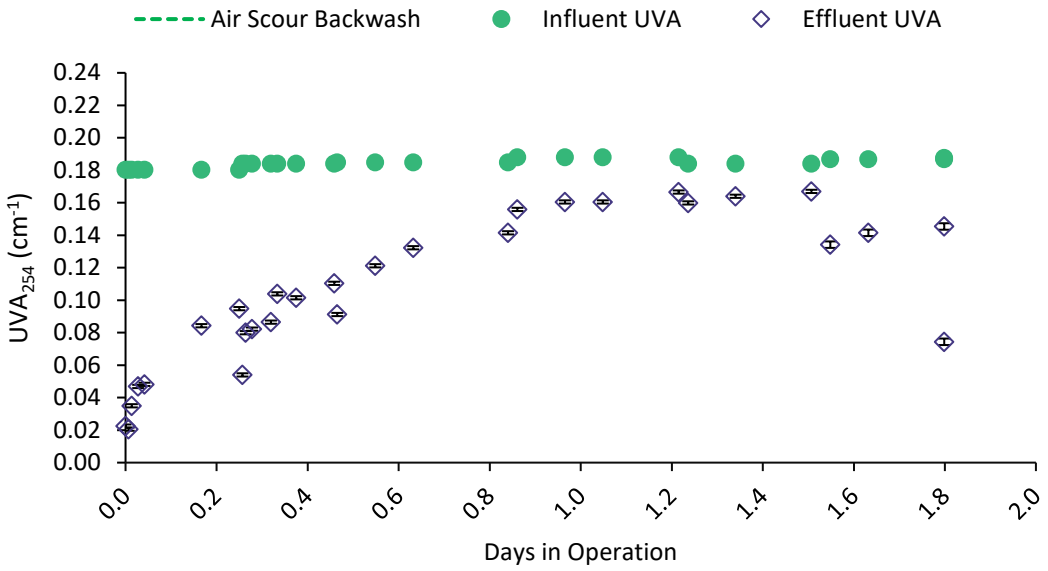

Figure 5-2: UVA_{254} influent and effluent values for the GAC column during the first two days of operation, before continuous operation began.

Figure 5-3 shows the influent and effluent UVA_{254} over the column lifetime, with continuous operation from day 9 onwards. The influence of temperature was apparent, as influent UVA_{254} values increased through the fall and was the highest in winter, with an average UVA_{254} of 0.197 ± 0.000 cm^{-1} between 165 and 278 days (December 2020 to April 2021). The inlet UVA_{254} during this time was 0.206 ± 0.000 cm^{-1}. The effluent UVA_{254} decreased through the spring due to the increase in temperature and biological activity, averaging 0.165 ± 0.000 cm^{-1} between 340 and 428 days (June to September 2021). The average influent UVA_{254} during this time was 0.186 ± 0.001 cm^{-1}. Both the influent and effluent UVA_{254} peaked on February 8th, 2021, which may indicate a change in the raw water composition. The gap in Figure 5-3 was due to Christmas break, when the operator was away; no sampling was performed and the column remained operational.

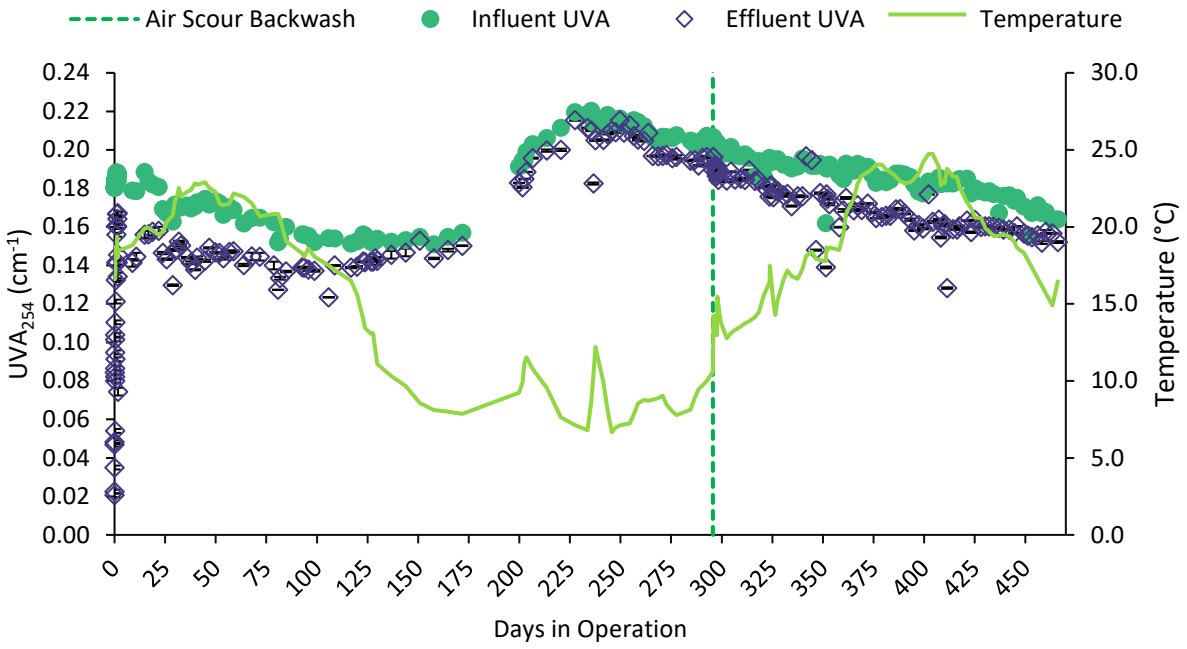

Figure 5-3: UVA_{254} influent and effluent values for the GAC/BAC column over 466 days of operation with temperature trend.

5.2 Ion Exchange (IEX) / Biological Ion Exchange (BIEX)

5.2.1 Dissolved Organic Carbon (DOC) Removal

During the first three days of the IEX experiment, six empty bed contact times (EBCT) were tested to examine the effect of EBCT step changes on DOC removal. EBCT changes between 7.5, 15, and 30 min, along with temperature, have been shown to have an impact on BIEX DOC removal performance (Liu et al., 2022), and small EBCT changes between 1, 2, and 3 min were seen to have significant impact on per- and polyfluoroalkyl substances (PFAS) removal (Murray et al, 2021). The EBCTs tested were 1.74, 3, 5, 6, 7, and 8 min. Figure 5-4 shows that there was very little significant impact on the effluent DOC concentration with a step change in EBCT.

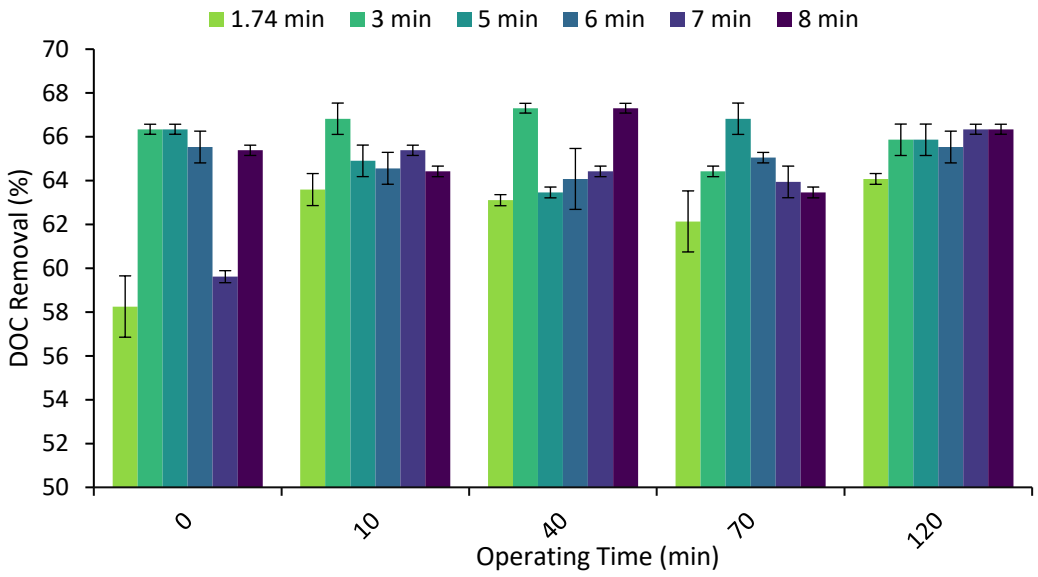

Figure 5-4: Comparison of DOC removal for various EBCT tests during the first two days of IEX operation.

The DOC removal for the 1.74 min EBCT was lower than the other five EBCTs as expected due to the decrease in contact time with the IEX resins. On performing analysis of variance (ANOVA), inclusion of the 1.74 min EBCT data suggested that there was significant difference in the DOC removal for each EBCT ($F = 3.33 > F_{crit} = 2.62$, $\alpha = 0.05$). However, an ANOVA performed excluding the 1.74 min EBCT data returned no significant difference between the 3, 5, 6, 7, and 8 min EBCT DOC removals ($F = 1.34 < F_{crit} = 2.87$, $\alpha = 0.05$). For Purolite A860, the manufacturer recommends an operating flow of 8-16 BV/h, corresponding to a EBCT range of 3.75 – 7.5 min for this system (Purolite, 2021). It is suggested that the EBCTs tested between 3 – 8 min showed no difference as they were either close or within the recommended operating range, which was likely optimized to balance the improvement in mass transfer with the decrease in treatment media contact time as flow rate increases.

Figure 5-5 shows the influent and effluent DOC concentrations for the BIEX column which operated from May 27th, 2020, to October 5th, 2021, approximately 465 days or 45,000 BV.

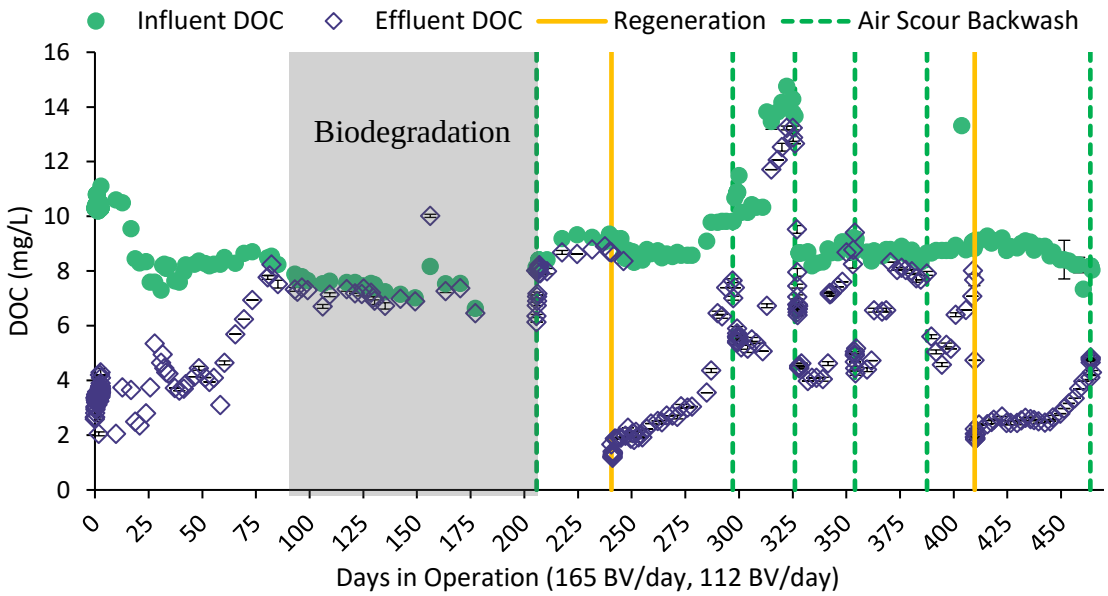

Figure 5-5: DOC concentration in the influent and effluent of the BIEX column over 465 days.

The influent DOC concentration ranged between 6.6 ± 0.1 mg/L and 14.8 ± 0.2 mg/L, averaging 9.1 ± 0.1 mg/L. Also, shown are the vigorous air scour backwashes and regenerations that were performed over the research period, described in sections 4.4.3.3 and 4.4.3.4. For clarity, regular backwashes are not shown; however, they occurred weekly. The influent DOC concentration spike on day 322 (May) was likely due to lake turnover, which released nutrients and organics that had settled on the bottom of the lake. At the start of operation, the DOC effluent concentration averaged 3.4 ± 0.1 mg/L, and was the lowest on day 2 (June 3rd, 2020), at 2.1 ± 0.1

mg/L. The lowest effluent DOC concentration after the first regeneration was 1.2[1] mg/L and 1.9 ± 0.0 mg/L after the second regeneration. Although the GBID source water had 2.0 mg/L higher influent DOC, these effluent DOC values are in line with what was seen in the Pont-Viau pilot study in Laval, both at the start and after regeneration (Amini et al., 2018). This could be due to differences in NOM characteristics between the source waters: if the NOM from Cranby Lake differed in charge density or molecular weight compared to the NOM from Jericho Pond, it could lead to a higher DOC removal, as Bazri et al. reported (Bazri et al, 2016; Bazri & Mohseni, 2016). Effluent DOC varied as the column progressed through primary and secondary IEX, and finally increased to near influent level as biodegradation took over.

It is interesting to note that after an air scour backwash, the effluent DOC concentration decreased temporarily, before returning to pre-backwash concentrations. This was unexpected, as adding air scouring to backwash was not seen to have an effect in BAC operations (Emelko et al., 2006). This phenomenon will be discussed in detail in section 5.2.1.2.

It appeared that biodegradation had minimal contribution to the removal of DOC, with effluent DOC averaging 7.6 ± 0.1 mg/L during the time when both primary and secondary IEX had ended, highlighted in Figure 5-5 in grey. Treated water TOC concentrations should not exceed 4.0 mg/L according to the BC source drinking water guidelines, so biodegradation alone is not sufficient for treating Cranby Lake source water (B.C. Ministry of Environment and Climate Change Strategy, 2020). Between September 10th, 2020, and January 13th, 2021, after which the air scour backwash may have influenced DOC removal, the average BIEX DOC removal per volume of treated water per minute was 0.89 ± 0.12 %/L/min, while the BAC DOC removal per volume of treated water per minute was 2.74 ± 0.31 %/L/min.

[1] Error unknown due to missing instrumental report

Figure 5-6 shows the DOC removal per volume of treated water per minute for both BAC and BIEX between days 81 and 130. Of the 13 days when sampling coincided, BAC had significantly higher DOC removal than BIEX for 11 days, while the remaining two days showed no difference.

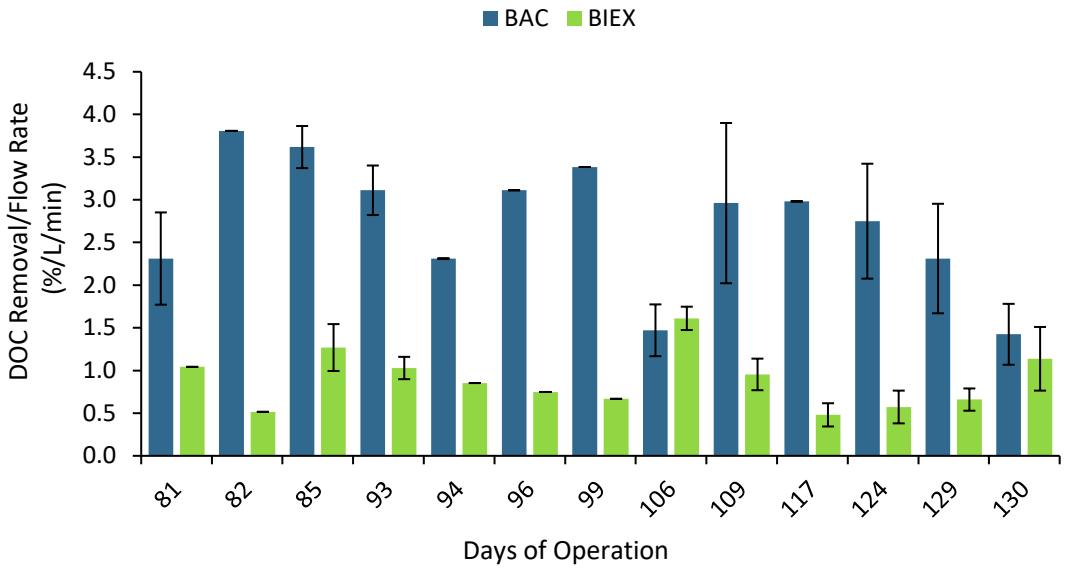

Figure 5-6: DOC removal per unit volume per time for BIEX and BAC columns between 80 and 238 days of operation.

The graphical results and the average DOC removals per volume of treated water per minute for each column suggest that there is a significant difference between the biodegradation of DOC in the BIEX and BAC columns. On performing an independent t-test to assess the difference between the BAC and BIEX average DOC removals per volume of treated water per minute, the results were significant at 95%. Li et al. (2017) reported that, in a single treatment train, there was a significant difference in the microbial communities between BAC and sand filters (Li et al., 2017). On the sand filter they reported that between 4.4 – 14.4 % of the phyla present was *Acidobacteria* while the BAC filter had 12.2 – 30.0 % *Acidobacteria*. They reported that the

filter media appeared to select for surface-associated bacteria, as indicated by the difference between influent and effluent Operational Taxonomic Units (OTUs). As Li et al (2017) reported that the filters appeared to select for surface-associated bacteria, it is possible that the microbial communities in the BAC and BIEX columns could differ in composition due to the vast differences between the BAC and BIEX resin substrates, such as surface area, particle size, and bed porosity (Crittiden, 2012). These substrates could support the growth of biofilm in different ways, leading to different microbial communities and affecting DOC removal. To properly determine the difference between the biofilm composition on BAC and BIEX filters, biofilm collection and RNA sequencing would need to be performed alongside DOC removal testing.

5.2.1.1 UV Absorbance at 254 nm (UVA_{254})

Figure 5-7 shows the influent and effluent UVA_{254} of the BIEX column over its 465-day operational lifetime. The influent UVA_{254} averaged around 0.166 ± 0.001 cm^{-1} for 177 days, between the start of operation and December 14th, 2021. After this time, it rapidly increased to a maximum of 0.219 ± 0.001 cm^{-1} by day 251 (February 27th, 2021). The influent UVA_{254} showed no large change on day 322 (May 2021) when the influent DOC concentration spiked from lake turnover, as discussed in section 5.2.1. It is possible that the organic matter composition of the lakebed was different than what was seen during the first year of operation, having a higher concentration of DOC yet a similar concentration of UV-absorbing compounds. This can be seen by looking at the specific UV absorbance (SUVA). The SUVA averaged 2.08 ± 0.02 L/(mg C·m) over the research period, however dropped to average 1.45 ± 0.02 L/(mg C·m) between day 311 and 325, which may indicate a small decrease in aromaticity and a change in NOM composition (Weishaar et al., 2003).

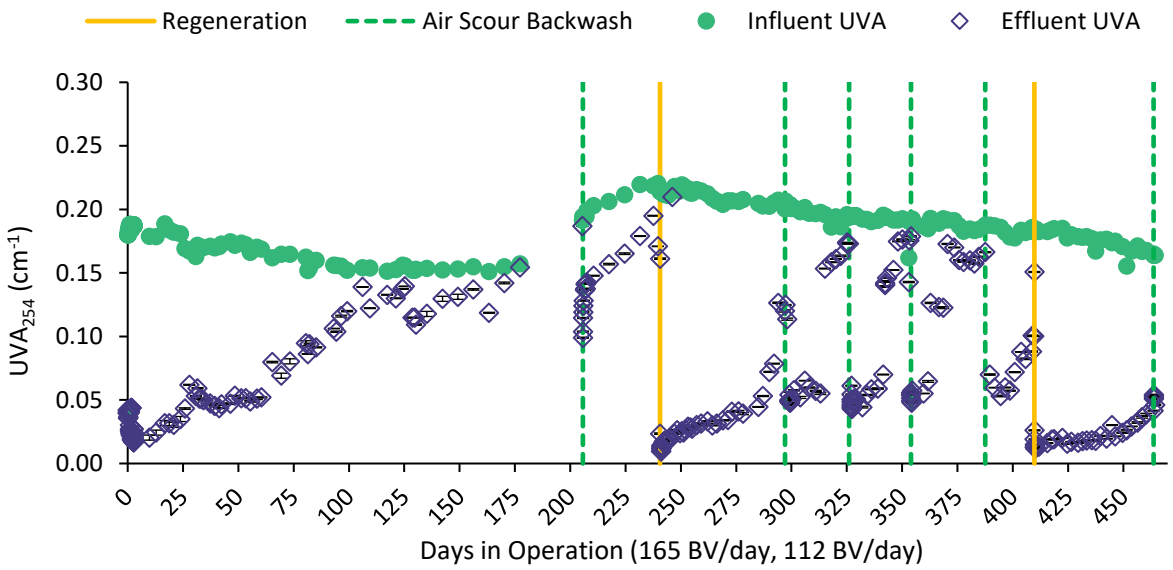

Figure 5-7: Influent and effluent UVA_{254} for the BIEX column over its lifetime of 465 days, showing regenerations and air scour backwashes.

The effluent UVA_{254} started low and was low after each regeneration, at 0.042 ± 0.002 cm^{-1}, 0.024 ± 0.000 cm^{-1}, and 0.026 ± 0.000 cm^{-1}, respectively, and these values agreed with Amini et al.'s findings (Amini et al., 2018). Accordingly, the UVA_{254} improvement was also greatest at the start of operation and after each regeneration. Low UVA_{254} values were expected after a regeneration, as the active sites were reloaded with chloride ions and primary IEX commenced once again to remove UV-absorbing compounds. There was also a drop in effluent UVA_{254} after each air scour backwash due to the increased removal of UV-absorbing compounds alongside the increased DOC removal discussed in section 5.2.1. After the first air scour backwash that took place during resin extraction on January 13th, 2021, the UVA_{254} improvement increased from 2.5 ± 0.1% the morning before backwash to 49.1 ± 0.2% the morning after. It was suspected that this improved UVA_{254} removal was caused by the air scour backwash prolonging the secondary IEX phase, and this finding provoked testing of multiple air scour backwashes during phase 3. The air scour backwash phenomenon will be discussed further in section 5.2.1.2.

5.2.1.2 Backwash

Figure 5-8 shows the DOC removal and UVA_{254} improvement during the time when air scour backwashing was performed, from day 170 prior to the February 17th regeneration to day 470.

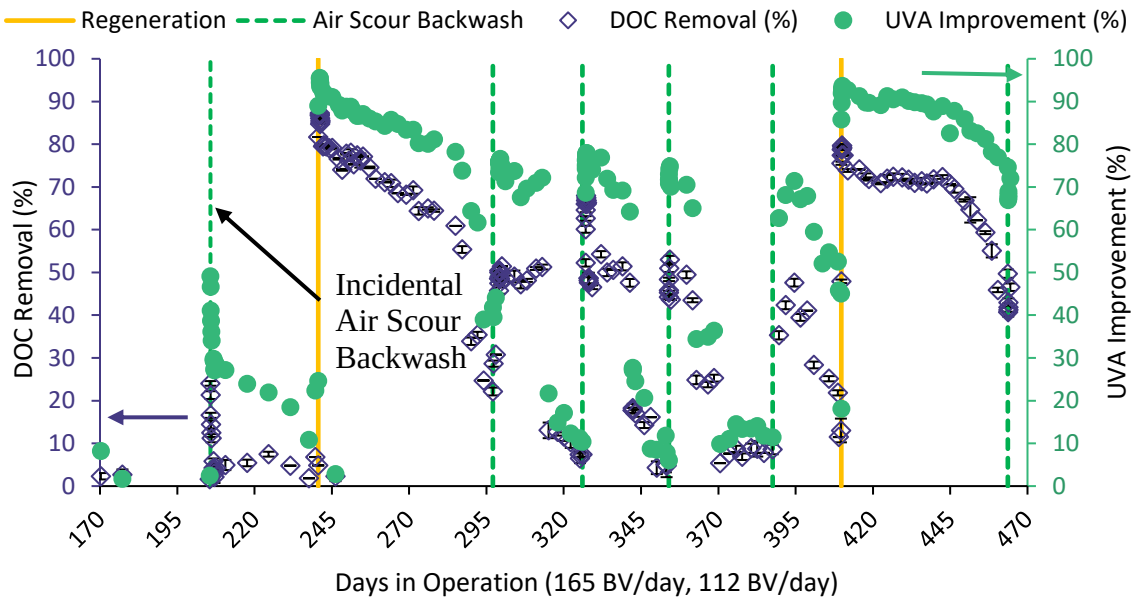

Figure 5-8: DOC removal and UVA_{254} improvement for the BIEX column during the time when air scour backwashes were performed, from day 170 to 470.

During resin extraction on day 206 (January 2021), introduction of air into the column was used to return the column head to its proper position. Samples taken immediately after this occurrence showed decreased concentration of DOC in the effluent. The DOC removal had improved from 1.0 ± 0.7% prior to resin extraction to 23.6 ± 0.5% the morning after, and the UVA improvement had increased to 49.1 ± 0.6 % from 2.5 ± 0.7%. This increase lasted one day; by the morning of January 14th, 2021, the DOC removal and UVA improvement were down to 5.8 ± 0.6% and 29.7 ± 0.6% respectively. During Phase 3, air scour backwashes were implemented regularly to

explore this phenomenon. Immediately after an air scour backwash, both the DOC removal and the UVA_{254} improvement increased temporarily. These results are summarized in Table 5-1.

Table 5-1: DOC Removal and UVA_{254} Improvement Comparisons for Air Scour Backwash Events

	Day of Backwash Event				
	297	**326**	**354**	**388**	**464**
Pre-BW DOC Removal (%)	22.1 ± 0.9	7.4 ± 0.5	4.8 ± 2.7	8.6 ± 1.1	45.9 ± 0.5
Post-BW DOC Removal (%)	51.4[2]	68.0 ± 0.3	53.0 ± 0.9	47.6 ± 0.9	49.7 ± 1.0
Pre-BW UVA_{254} Improvement (%)	39.0 ± 0.6	10.4 ± 0.7	6.0 ± 0.7	11.4 ± 0.7	76.9 ± 0.6
Post-BW UVA_{254} Improvement (%)	76.6 ± 0.5	77.9 ± 0.5	74.8 ± 0.5	67.9 ± 0.6	74.6 ± 0.6

Aside from the final air scour backwash, there was consistent improvement in the removal of DOC and in the decrease of UV-absorbing compounds, showing a significant impact of adding air scour into the backwash procedure. For the final air scour backwash, there was a slight increase in the DOC removal and a decrease in the UVA_{254} improvement, suggesting that this air scour backwash had no or little effect on the removal capacity of the BIEX column. The major difference between this backwash and the others is that the column was still operating in primary IEX, where the other four air scour backwashes took place when the column was operating in secondary IEX. Also seen was the consistent diminishment in DOC removal and UVA_{254} improvement after each backwash, suggesting that there is a limit to the number of times this phenomenon could be used to improve effluent water quality, which will be of particular importance to operators in the field. As the weekly water backwashes had no significant effect on

[2] Error unknown due to missing instrumental report

the effluent water quality, the quality improvement could be attributed to the air scouring of the column, however the gradual decrease in water quality improvement suggests that the improvement may not be directly attributed to the air scour, but instead facilitates an improvement mechanism.

5.2.1.3 BIEX DOC Removal – Total Resin Exhaustion

In previous studies, laboratory or pilot scale tests have progressed into secondary IEX but may not have reached secondary IEX exhaustion (Amini et al., 2018; Liu et al., 2020, 2022; Schulz et al, 2017). In phases 1 and 2, which ran from day 1 to day 241, secondary IEX was exhausted by day 81 (September 10th, 2020), reaching an estimated DOC loading of 0.62 eq/L, 78% of the maximum theoretical capacity of 0.8 eq/L. In the first part of phase 3, which ran from day 241 to 410, secondary IEX was exhausted around day 406 (August 6th, 2021), 165 days after regeneration, and reached an estimated DOC loading of 0.45 eq/L, 58% of the maximum theoretical capacity. The differences between DOC loaded and time to secondary exhaustion depend on many factors, such as backwashing method, and is explored in this section through inorganic ion analysis and overall resin saturation.

5.2.2 Inorganic Anion Analysis

5.2.2.1 Chloride Release

Figure 5-9 shows the chloride released from the IEX/BIEX column over its lifetime of 465 days.

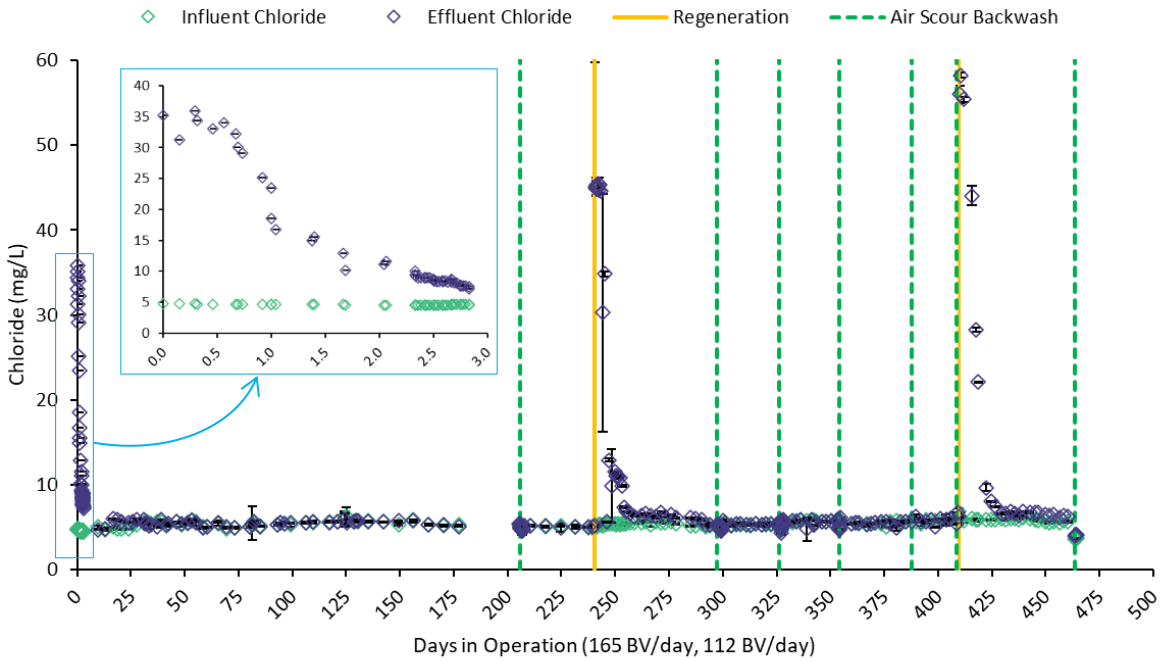

Figure 5-9: Influent and effluent chloride concentrations showing chloride release from the IEX/BIEX column over its lifetime, 465 days.

A spike in effluent chloride concentration occurred at the start of operation, corresponding to the initial chloride loading of the fresh ion exchange resins. Regeneration, which occurred on day 241 and day 410, corresponded with the large chloride effluent spikes that resulted from the displacement of chloride ions by NOM and sulphate ions during primary IEX operation. The peak concentrations of chloride at the start of operation, one BV after the first regeneration, and

one BV after the second regeneration were 35.18[3] mg/L, 60.17 ± 0.37 mg/L, and 143.21 ± 6.52 mg/L, respectively. The differences in chloride loading will be discussed further in sections 5.2.2.2.2 and 5.2.2.2.3. During Liu et al.'s study, chloride was exhausted within 1000 BV and in the study performed by Amini et al., chloride was exhausted by 4800 BV; in this research, the chloride in the BIEX column was exhausted after 2200 BV (10 days) in June 2020 (Amini et al., 2018; Lu et al., 2020). After regenerations 1 and 2, the chloride was exhausted after 1500 BV (19 days) and 1200 BV (20 days), respectively. These differences in times to initial chloride exhaustion may be related to EBCT and DOC concentration, as Amini et al. had a high EBCT and DOC concentration, while Liu et al. had a low EBCT and low DOC concentration, and this study had a low EBCT with a high DOC concentration. Post-regeneration chloride exhaustion time would be affected by EBCT; however, it could also be affected by biofilm accumulation: regeneration 1 was backwashed without air scour, likely removing less biofilm, hindering access to ion exchange sites, and increasing time to primary IEX exhaustion. Time to exhaustion could also be impacted by changes in resin structure over time from resin swelling and kinetics changes due to cyclical temperature trends.

5.2.2.1 Sulphate Release

Figure 5-10 shows the influent and effluent concentration of sulphate over the lifetime of the BIEX column, 465 days; the influent sulphate concentration averaged 2.88 ± 0.13 mg/L. At operation start and after regeneration, effluent sulphate concentration dropped to undetectable levels due to adsorption: sulphate is removed by displacing chloride and NOM fractions according to affinity differences during primary ion exchange, as Liu et al. described (Liu et al.,

[3] Error unknown due to missing instrumental report

2020). As primary IEX proceeded, the available active sites became saturated with sulphate and DOC, resulting in residual effluent sulphate. After primary IEX was complete, a switch from sulphate adsorption to sulphate release occurred, indicating that secondary IEX was underway. Sulphate release and secondary IEX started on the 32nd day of operation (July 12th, 2020), slower than the 10 days seen by Liu et al., yet sooner than the estimated 90 days seen by Amini (Amini et al., 2018; Liu et al., 2020). The effluent sulphate concentration peaked on day 37 (July 27th, 2020) at a concentration of 5.99 ± 0.06 mg/L, and release continued until day 81 (September 10th, 2020), while Liu et al. saw continued sulphate release until past day 250, possibly due to the higher influent sulphate concentration, at 28.2 ± 4.5 mg/L (Liu et al., 2020). Using the Aspen-Welch t-test, the effluent sulphate concentration was not significantly different from the influent concentration at a 95% confidence level between day 94 and 206 (when air scour occurred), confirming the end of secondary IEX.

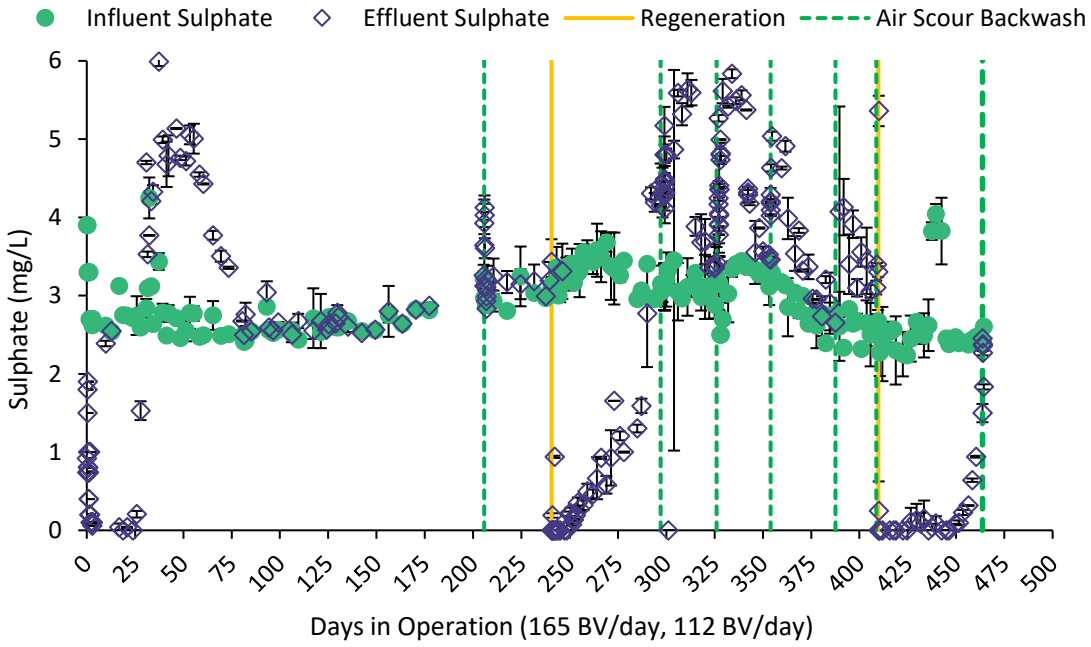

Figure 5-10: Influent and effluent sulphate concentration, showing the adsorption and release of sulphate in the IEX/BIEX column over its lifetime, 465 days.

The amount of sulphate in the effluent was significantly higher than the influent concentration immediately after an air scour backwash, indicating that sulphate release was occurring once again. On day 206 (January 13th, 2021), an incidental air scour backwash took place during maintenance. Immediately after this introduction of air, the effluent sulphate concentration increased from being 2% higher than the influent concentration to peak at 4.12 ± 0.16 mg/L sulphate in the effluent, 28% higher than the influent concentration. This corresponded with an increase in DOC removal. After the first regeneration, effluent sulphate concentrations slowly increased until day 290 (April 12th, 2021) when secondary IEX started. Table 5-2 shows the effluent concentration of sulphate at its peak following each air scour backwash.

Table 5-2: Peak Effluent Sulphate Concentrations

Backwash Day	**Day of Peak Effluent Concentration**	**Number of Days to Peak**	**Effluent Sulphate Concentration** (mg/L)
297	299	3	5.17 ± 0.24
326	334	8	5.84 ± 0.01
354	355	1	5.04 ± 0.06
387	391	4	4.13 ± 0.36

The time until the peak effluent sulphate concentration ranged between 1 and 8 days, which could have many contributing factors. The average influent DOC concentration was the highest prior to the second backwash, at 11.89 ± 0.08 mg/L, potentially contributing to a larger buildup of biofilm, and while the conditions of air scour backwash were controlled, it is not possible for each air scour backwash to have been identical due to uncontrolled hydraulic conditions inside the column, coarse control of airflow into the column, and potential air leakage. The final air scour backwash occurred on day 463 (October 4th, 2021) and showed no discernable sulphate release; sulphate was still being adsorbed. It is suspected that the DOC removal improvement that followed an air scour backwash was facilitated by a release of previously inaccessible sulphate ions which had remained in resin pores due to pore blockage from biofilm growth. As water flow would take the path of least resistance, higher resistance to flow due to biofilm could cause channeling in the media, preventing diffusion and reducing the effectiveness of ion exchange, as proposed by Edgar & Boyer (Edgar & Boyer, 2021). The final air scour backwash took place before any sulphate release had taken place and so, rather than a release of ions, adsorption simply resumed after backwash.

5.2.2.2 Resin Saturation

By measuring the concentration of DOC, chloride, nitrate, and sulphate in the influent and effluent streams, the anion loading of the resins was quantified. A mass balance was calculated on each individual ion per sample, and the amount loaded or released was converted from mg to equivalents per unit volume (eq/L). The charge densities of the compounds of interest in this research are outlined in Table 5-3.

Table 5-3: Charge Densities of Compounds of Interest

Compound	**Charge Density** (mEq/g)
Chloride	28.21
Nitrate	16.13
Sulphate	20.82
Alkalinity (as $CaCO_3$)	19.98
DOC	10.16*

* Charge density of NOM assumed to be the same as for Suwannee River NOM, as calculated in (Bazri, et al, 2016).

Loading of alkalinity was not used to determine resin saturation due to large instrument error as no valuable insight was gained.

5.2.2.2.1 Phases One & Two: Commissioning to First Regeneration

Figure 5-11 shows the cumulative resin saturation over the first 241 days, from May 27th, 2020, to February 16th, 2021. The light green line at the top indicates the theoretical maximum capacity of the resins based on the equivalent data given by the manufacturer.

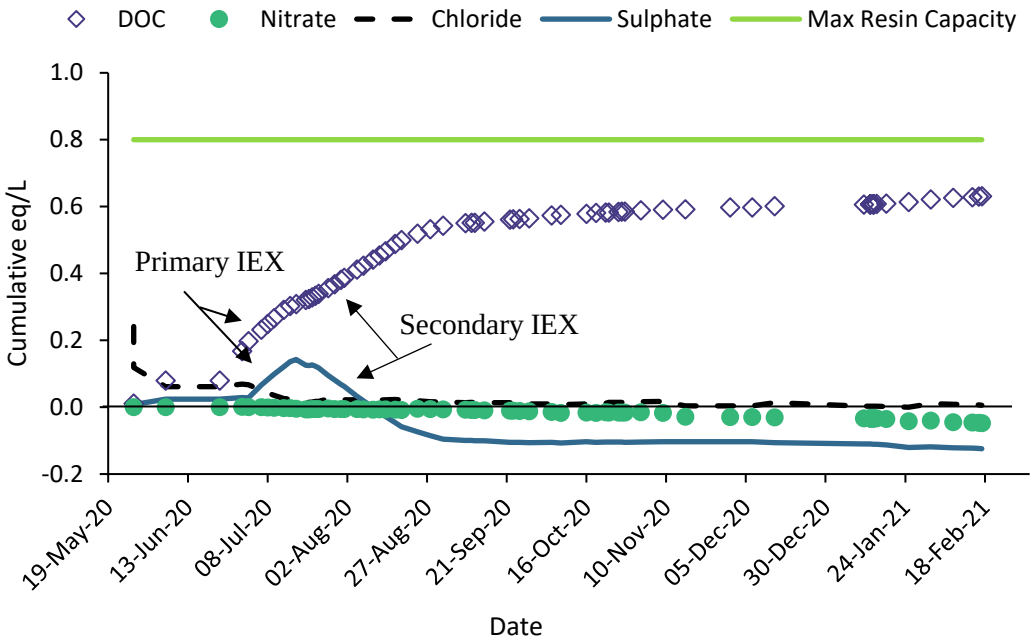

Figure 5-11: Resin saturation of IEX resins from May 27th, 2020, to February 17th, 2021.

The increase in loaded DOC shows that the IEX resins were performing as expected to remove DOC from water. The initial loading of DOC and sulphate coincided with chloride release: primary IEX. Once the sulphate finished loading and began to release, another significant increase of loaded DOC occurred: secondary IEX. As the sulphate release plateaued, the apparent loading of DOC continued slowly, suggesting that biodegradation continued to remove DOC. The total DOC loaded was 0.63 eq/L, 79% of the theoretical maximum of 0.8 eq/L. Total sulphate and nitrate loading both fell below zero, suggesting that more ions were released than were loaded. This could be due to instrumental error, incorrectly assuming 100% loading of virgin resins, or start-up issues, but this occurrence is not uncommon, as Zimmermann et al. reported similar results (Zimmermann et al, 2021). The maximum cumulative chloride released was 0.24 eq/L, suggesting that this was the total chloride available for primary IEX. At the end of primary IEX, 0.14 eq/L of sulphate and 0.31 eq/L of DOC had been loaded, suggesting that

there was a total of 0.45 eq/L chloride exchanged during primary IEX, far greater than the maximum seen released. This discrepancy may be due to the charge density of DOC, as it was assumed to be 10.16 mEq/g, the charge density of Suwannee River NOM, and may not have been representative of the NOM in the GBID source water.

Research has previously showed that there is much variation in the charge densities of fulvic and humic acids for different waters; and Bazri & Mohseni (2016) showed that Suwannee River fulvic acid had a charge density of 10.97 mEq/g, while Suwannee River humic acid had a charge density of 8.89 mEq/g; thus, different compositions of fulvic and humic acid in water would significantly change the overall NOM charge density (Bazri & Mohseni, 2016; Ma, Allen, & Yin, 2001; Ritchie & Michael Perdue, 2003).

Additionally, there could have been DOC removed due to simple adsorption instead of ion exchange. A full characterization of Cranby Lake NOM would have resulted in more accurate DOC results; however, this task could not be performed during this research due to instrument accessibility limitations. Surface water is estimated to have a natural ammonia concentration below 0.2 mg/L, so the discrepancy in nitrate loading could be explained by the presence of ammonium in the raw water being nitrified biologically in transport (WHO, 2022). This phenomenon could not be confirmed as ammonia tests returned below detectable range due to ammonia being present as ammonium at neutral pH, and no pH buffering was performed.

5.2.2.2.2 Phase Three: First Regeneration to Second Regeneration

Figure 5-12 shows the resin saturation after the first regeneration on February 17th, 2021, until the second regeneration on August 10th, 2021, a total of 169 days.

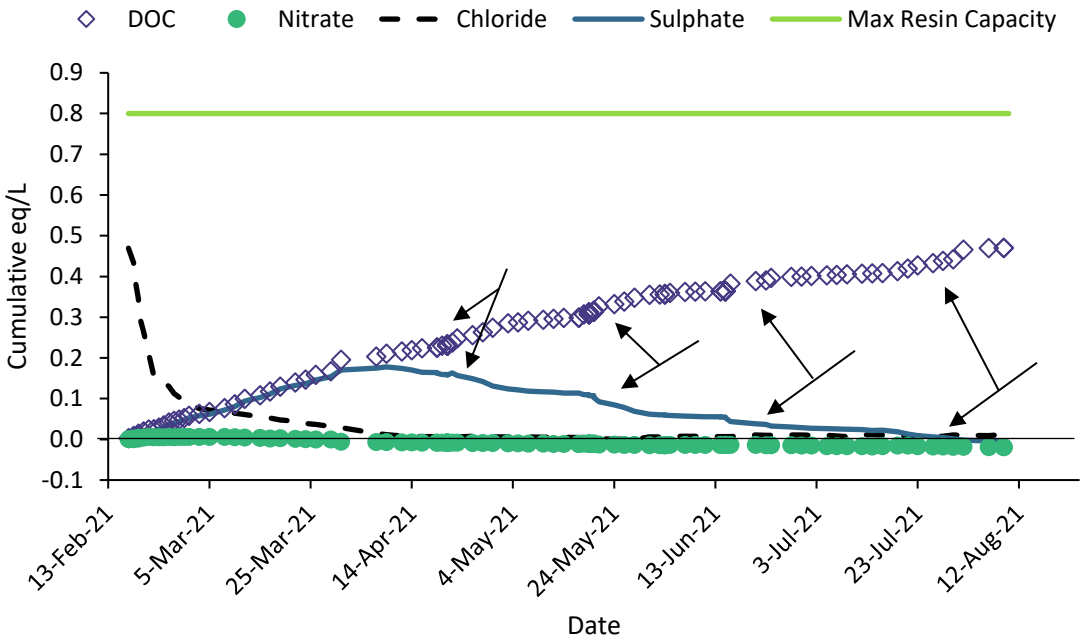

Figure 5-12: Resin saturation for IEX resins from February 17th, 2021, to August 10th, 2021, with arrows indicating dates of air scour backwashes.

The IEX resins were regenerated on February 17th, 2021, and according to the maximum calculated chloride released, was loaded with 0.47 eq/L of chloride, 59% of the theoretical maximum of 0.8 eq/L. This low chloride loading suggests that the regeneration performed in February 2021 may not have reloaded the active sites completely, potentially due to an insufficient regeneration sequence which consisted of four regeneration cycles of 60, 70, 70, and 40 min, with one 105-minute soak after the first cycle. Additionally, biofilm accumulation or channelling present in the column undisturbed by the water-only backwash performed prior to regeneration could have reduced access to active sites, contributing to the poor reloading of chloride. The low loading seen could also have been caused by biofilm accumulation after regeneration, blocking access to the pore matrix containing chloride ions and reducing IEX

efficacy. The kinetics of regeneration may also have been reduced by the low ambient temperature, as seen by Liu et al. (Liu et al., 2022).

Interestingly, the DOC and sulphate loaded during primary IEX are similar and loaded at an average ratio of 1.1:1 DOC to sulphate, suggesting that the resins had a similar affinity for both DOC and sulphate at the concentrations found in GBID water. Primary IEX loaded 0.21 eq/L of DOC and 0.18 eq/L of sulphate, after which the sulphate released in secondary IEX with a ratio of 2.0:1 DOC loaded to sulphate released. Sulphate was exhausted around day 406 (August 2021), and it is suspected that only biodegradation would have removed DOC after this point.

On August 9th, prior to regeneration, there was a total of 0.47 eq/L DOC loaded on the resins, equal to the estimated initial chloride loaded and agreeing with Lui et al.'s evidence of chloride being displaced mainly by NOM and sulphate (Liu et al., 2020). Nitrate and sulphate were not included in the total resin loading on August 9th as they were both reported to be below zero at this point. Again, more nitrate was released than was loaded. This was hypothesized in section 5.2.2.2.1 to be due to biofilm performing ammonium nitrification, as surface water can have background ammonium concentrations of less than 0.2mg/L, although ammonium concentrations were not analysed (WHO, 2022).

In phase three, air scour backwashes were implemented regularly during secondary IEX. Each air scour backwash caused a release of sulphate and a corresponding increase in DOC loading, indicated with black arrows in Figure 5-12. As proposed in section 5.2.1.2, the air scour backwash appeared to have facilitated the extension of secondary IEX operation by exposing sulphate-loaded active sites for ion exchange, possibly through the disturbance of resin

aggregates and accumulation of biofilm blocking access to the pore matrix, as seen by Edgar & Boyer (Edgar & Boyer, 2021).

5.2.2.2.3 Phase Three: Second Regeneration to Decommissioning

Figure 5-13 shows the resin saturation after the second regeneration, from August 11th, 2021, to the end of the pilot study on October 4th, 2021.

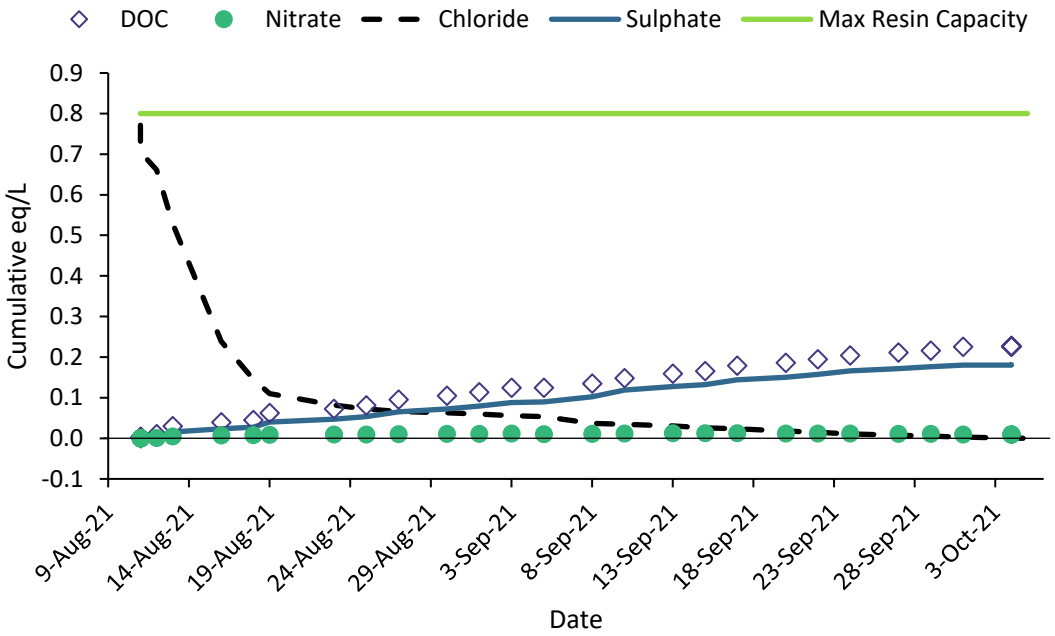

Figure 5-13: Resin saturation for IEX resins from August 11th, 2021, to October 5th, 2021.

The initial chloride loaded was much higher than it was at operation start in May 2020 or after the first regeneration in February 2021, with the maximum chloride loaded in August 2021 being approximately 0.77 eq/L, 96% of the resin capacity. The increase in chloride loaded is substantial and supports the theory that the February regeneration may have been ineffective at

fully reloading the active sites with chloride ions, as only 59% of the theoretical chloride loading was reached compared to 96% in August.

The regeneration performed on August 11th had a different sequence than the one performed in February: 60 min regeneration, 10 min rinse, two 60 min regenerations, a 16-hour soak, three 60 min regenerations, and one 10 min rinse; active regeneration occurred over 6 hours. As seen by Bazri et al, regeneration was seen to have been more effective when using a sequence of three 30 min regenerations compared to one 2-hour regeneration, supporting the suggestion that the approach of the second regeneration may have been more effective (Bazri et al, 2016). This sequence was also immediately preceded by an air scour backwash, which would have removed more biofilm and disturbed aggregate resins more effectively than the water only backwash performed on February 17th, suggesting that these issues may either have had a significant effect on the reloading of chloride ions during regeneration, or reducing efficacy of subsequent IEX. Additionally, the ambient temperature at this time was 24.8 ± 0.5°C, compared to 11.5 ± 0.5°C in February, which may have resulted in improved regeneration kinetics.

Once again, the DOC and sulphate loading was comparable with an average ratio of 1.1:1 DOC to sulphate, suggesting the resins had similar affinity for both DOC and sulphate. At the end of this experiment, nitrate release was consistent with nitrate loaded, unlike what was seen earlier. If additional nitrate release was due to biological ammonium nitrification as proposed earlier, this difference could have been caused by the biofilm not being fully established yet, only 35 days after the end of chloride release, as ammonium nitrifiers have slow growth kinetics (Rittmann & McCarty, 2001).

Chapter 6: Laboratory Study Results and Discussion

Resins extracted regularly from the BIEX pilot column on site in GBID were shipped to UBC for use in multiple loading tests (MLTs) to explore remaining resin capacity. MLTs were also performed to assess the regeneration performed in GBID. For extracted resins, MLTs ran until the end of secondary IEX when sulphate was finished releasing, and virgin Purolite A860, hereafter named vA860, ran for 22,000 BV to correspond with regeneration MLTs. Mass transfer differences between the column test (a packed bed reactor) and MLTs (a stirred tank reactor) resulted in different kinetics and the inability to directly compare results from MLTs to the pilot experiment, but provided insight about resin saturation and conditions at the time of extraction (Gari-Grulovic et al., 2011). Conditions were set as outlined in section 4.5, based on previous evaluation within our lab, to simulate commercial suspended bed applications (Dixit, 2017). Each extracted resin sample was considered separately to examine the remaining capacity at time of extraction.

6.1 Dissolved Organic Carbon (DOC) Removal

DOC results from the MLTs were inconclusive, unlike the DOC removal results seen in Chapter 5:, and as such are not presented here. Winter et al., in his MLT experiments, saw a steady upward trend when comparing effluent and influent DOC concentration; however, the results from this research were not as clear (Winter et al., 2018). For vA860, the large variation in data was suspected to be mainly caused by issues with instrumental DOC analysis: while standard deviation between the three tests on a sample was often in the magnitude of 0.07 mg/L, one example sample had a standard deviation of 0.69 mg/L. This large variation introduced uncertainty into the DOC concentration values. For extracted resin samples, biofilm detachment

may have also contributed to data inconsistencies. Biofilm detachment may occur from erosion of biofilm due to shear forces from moving fluid, abrasion due to resin collisions, and sloughing of biofilm by random detachment (Chang et al., 1991; Nicolella et al., 1997). In those studies, effluent biofilm concentration was determined by analyzing the TOC and volatile suspended solids (VSS) to calculate detachment rates. VSS was not measured in this research, so it is not possible to compare influent and effluent suspended solids concentrations for biofilm detachment. The phenomena affecting DOC measurements did not appear to have an affect on UVA_{254} measurements. Biofilm detachment and cell decay leading to cell lysis could have released soluble, high MW-compounds into solution, which would affect DOC measurements yet affect UVA_{254} measurements to a lesser degree (Jarusutthirak & Amy, 2007).

6.1.1 UV Absorbance at 254 nm (UVA_{254})

Figure 6-1 shows the reduction in UV-absorbing compounds, reported as C/Co (effluent/raw UVA_{254}), for the June 6th, September 10th, February 16th, and vA860 resin MLTs. As the C/C_o values approached unity, the UVA_{254} effluent value approached that of the raw value, indicating decreasing removal of UV-absorbing compounds. Recall from section 4.5 that after each 1000 BV, the water was separated from the resins in the beaker and a new batch of raw water was introduced. As expected, the vA860 had the highest reduction in UV-absorbing compounds. The vA860 C/C_o started at 0.58 ± 0.00, followed by June, Sept, and Feb resins with starting C/C_o values of 0.69 ± 0.00, 0.88 ± 0.01, and 0.96 ± 0.01, respectively. These trends agree with what was seen during the pilot study and with what Amini et al. observed: as the column progressed through primary and secondary IEX to biodegradation, the removal of UV-absorbing compounds decreased (Amini et al., 2018). Bazri et al. reported similar trends for UVT: over

time, the number of UV-absorbing compounds in the effluent increased (Bazri et al., 2016). As the active sites filled, the resins were less effective at removing UV-absorbing compounds, suggesting a system where the removal rate was a function of the concentration of available active sites, as mentioned by Golub (Golub, 1957). The availability of active sites may be affected by the extent of adsorption occurred and pore blockage from either biofilm or previously adsorbed compounds (Bazri et al, 2016). The MLTs on Sept and Feb resins were concluded as results plateaued.

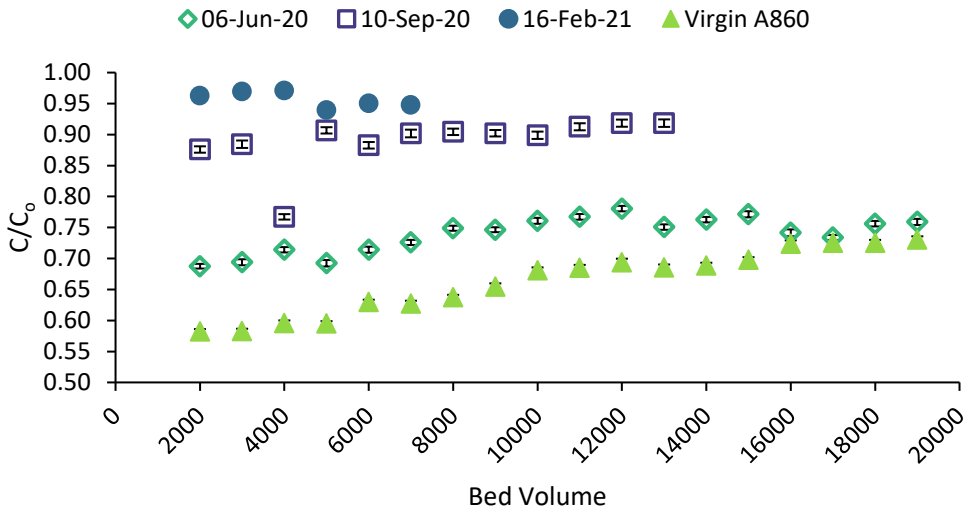

Figure 6-1: Effluent UVA254 normalized to raw UVA_{254} (C/C_o) for June 6th, 2020, September 10th, 2020, February 16th, 2021, and virgin Purolite A860 resins.

Figure 6-2 compares the reduction in UV-absorbing compounds, reported as C/C_o, between the on-site regenerated February 17th resins (OS-Regen) and the in-lab regenerated February 16th resins (L-Regen), against the vA860 resins.

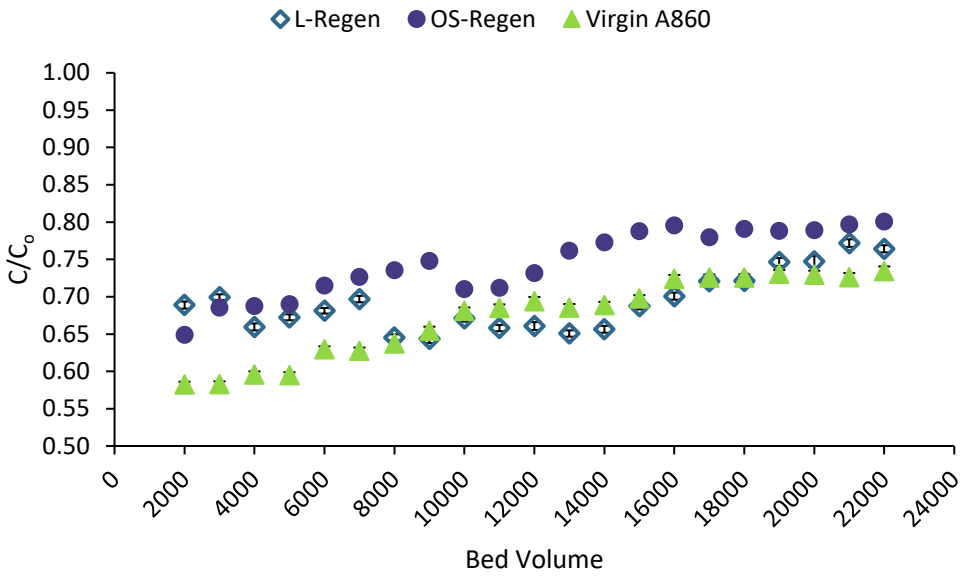

Figure 6-2: Effluent UVA_{254} normalized to raw UVA_{254} (C/C_o) for the virgin A860, the on-site regenerated February 17th resins (OS-Regen), and the in-lab regenerated February 16th resins (L-Regen).

The vA860 initially had the highest reduction in UV-absorbing compounds, with a C/C_o of 0.58 ± 0.00, followed by the OS-Regen with 0.65 ± 0.00 and the L-Regen with 0.69 ± 0.00. After 3000 BV, the number of UV-absorbing compounds in the effluent of the OS-Regen tests became higher than what was seen in the L-Regen effluent, as seen in Figure 6-2 as a C/C_o closer to unity. On performing a t-test to examine the differences of C/C_o averages between each resin, it can be said with 95% confidence that there is no statistically significant difference between the L-Regen and the vA860; however, there is significant difference between the OS-Regen and both the L-Regen and the vA860. This shows that the OS-Regen resins were less effective at removing the UV-absorbing compounds than the vA860 or the L-Regen resins, while the L-Regen resins performed the same as the vA860. This could suggest that there was a difference in the efficacy of regeneration in reloading active sites with chloride ions, and subsequently sulphate ions, capable of removing UV-absorbing compounds, as less IEX would result in less removal. Difference in regeneration may have been due to the impacts on the kinetics of

regeneration on site, the kinetics of ion exchange, or both. If the kinetics of regeneration had been affected this could have been due to regeneration cycle inefficiencies, biofilm growth and channelling in the column undisturbed by the water-only backwash blocking access to active sites, and temperature effects. This phenomenon suggests the importance of regeneration scheme and indicates that optimization of regeneration requires research into the impacts of air scour backwash, temperature, number and length of cycles, and soaking time.

6.2 Inorganic Anion Analysis

6.2.1 Chloride Release

For the MLTs performed on the June, Sept, and Feb extracted resins, chloride release was negligible. As these resins were seen to have negligible amounts of chloride loaded on the date of their extraction, this result was expected, and indicated that no primary IEX was taking place. As expected, regeneration, on the other hand, showed release of chloride. Figure 6-3 shows the chloride release for the vA860, the lab regenerated resins (L-Regen), and the on-site regenerated resins (OS-Regen), calculated as cumulative chloride release in eq/L. While the data for 283 BV and 1000 BV cannot be used to evaluate any adsorption efficiency due to kinetics differences as the remaining tests all ran for 1000 BV, these data should be examined to determine the maximum chloride capacity of the regenerated resins. Rather than setting initial chloride loading to 0.8 eq/L, initial chloride loading was set to the maximum cumulative chloride released, as it was assumed that this value indicated the total chloride loaded at time of testing, resulting in a final chloride loading of essentially zero eq/L. All three resins

showed a chloride release greater than the theoretical resin capacity of 0.8 eq/L as provided by the manufacturer.

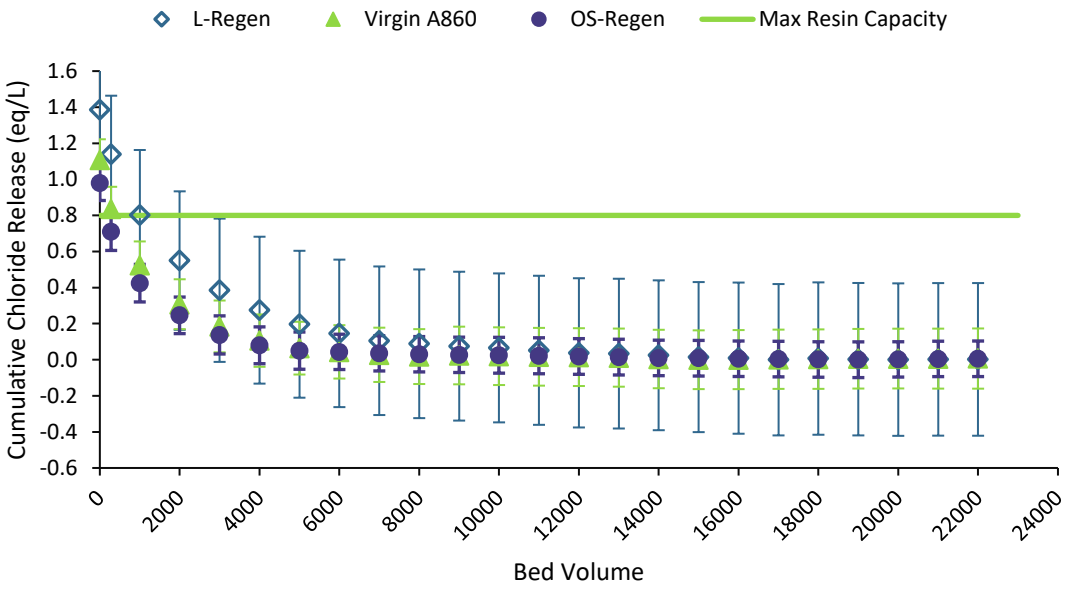

Figure 6-3: Chloride release from virgin A860 resins, in-lab regenerated February 16th (L-Regen) resins and on-site regenerated February 17th (OS-Regen) resins. Error bars show the cumulative error.

The L-Regen resins showed the greatest release of chloride at 1.4 ± 0.3 eq/L, followed by the vA860 and OS-Regen with 1.1 ± 0.1 and 1.0 ± 0.1 eq/L, respectively. These results indicate that all three resins were loaded with chloride ions to 100% capacity and disagree with the results seen in section 5.2.2.2.2, which suggested that the OS-Regen resins were loaded with 0.24 eq/L of chloride. As outlined in section 4.5.4, ten 5-minute rinses followed regeneration on the L-Regen and vA860 resins, while Zimmermann et al. performed extensive rinsing until the resulting supernatant contained less than 1 mg/L chloride (Zimmermann et al., 2021). Compared with the extensive rinsing performed by Zimmermann et al., it is possible that insufficient rinsing of the L-Regen and the vA860 resins artificially inflated chloride concentrations above the

theoretical maximum capacity due to chloride remaining in the pore matrix of the resins. For the OS-Resins, chloride inflation may also have been due to insufficient rinsing: the storage water keeping the resins hydrated from the pilot column had a salt concentration between 189 – 250 ppm and the only rinse occurred during resin vacuum drying before weighing.

Interestingly, the resins remaining in the column on site after the February regeneration saw a total chloride release of 0.47 eq/L, far below the maximum capacity of 0.8 eq/L, while the released chloride was much higher during MLTs. This may suggest a difference in resin capacity but may also be attributed to differing test conditions and will be examined in section 6.2.3.

6.2.2 Sulphate Release

Analysis was performed assuming no loading on extracted resins, to determine additional anion loading. As the extracted resins were stored for a minimum of 7 months in the column water that accompanied resins during extraction, it is possible that additional ion exchange took place within the falcon tube that cannot be accounted for. As such, the calculated anions loaded on the resins on extraction day was not used for estimation of total resin loading. Figure 6-4 shows the additional cumulative sulphate loading in eq/L for the June 6th, September 10th, February 16th, and virgin A860 resins. The vA860 resins act as a baseline to compare against.

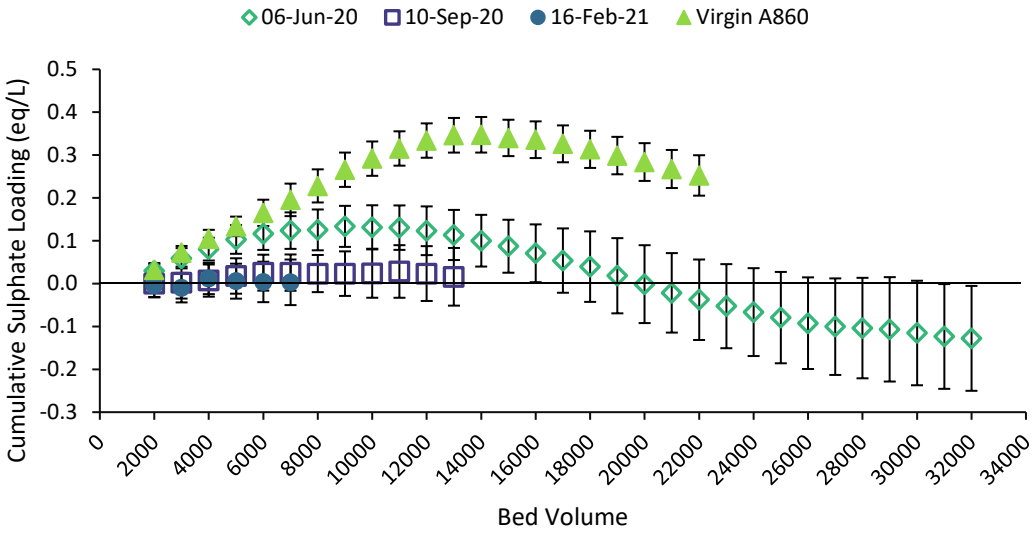

Figure 6-4: Cumulative sulphate loading for June 2020, September 2020, February 2021, and virgin A860 resins. Error bars show the cumulative error.

The June resins loaded 0.13 ± 0.05 eq/L of sulphate before release began. This suggests that primary IEX may still have been occurring on June 6th, as sulphate loads by displacing chloride and certain NOM fractions (Liu et al., 2020). After 32,000 BV, the June resins had released a total 0.26 ± 0.12 eq/L of sulphate, suggesting there was likely sulphate loaded onto the resins at the start of the MLTs; however, at time of extraction, there was an estimated 0.02 eq/L of sulphate loaded. This difference may be attributed to pore blockage from biofilm and resin aggregates, as discussed in section 5.2.2.2.2.

The Sept and Feb had negligible sulphate loading, which suggests that secondary IEX had ended by September 10th, and any affect on secondary IEX caused by the January air scour backwash had concluded by February 16th. As mentioned, there is a significant difference in the kinetics between the pilot (packed bed) and the MLTs (stirred bed). In the packed bed, the June resins were exhausted by Sept, running for an additional 9300 BV, while in the stirred bed secondary IEX appeared to have concluded after an additional 32,000 BV, indicating that

remaining filter life cannot be estimated from MLTs. The maximum sulphate loaded onto the pilot resins between June and February was 0.14 eq/L, which is within error of the sulphate released from the June resins in the MLTs. This suggests that a 1 mL resin sample may be able to predict the remaining sulphate capacity available for secondary IEX for the on-site packed bed column. However, the negligible sulphate loading seen in the Sept resins MLTs suggest that it may not be possible to determine the remaining sulphate loaded that could be utilized after an air scour backwash when equivalents loaded are low.

The results of the extracted resin experiments suggest that the information gained from MLTs may reflect the capacity of the columns, as Winter et al. saw no capacity change between MLT and column test, but also show that the data become less accurate as the mode of DOC removal approaches the end of secondary IEX, limiting its ability to determine if an air scour backwash would induce additional DOC removal (Winter et al., 2018).

Figure 6-5 shows the cumulative sulphate loading for the regeneration experiments between vA860, the lab-regenerated (L-Regen), and the on-site regenerated (OS-Regen) resins.

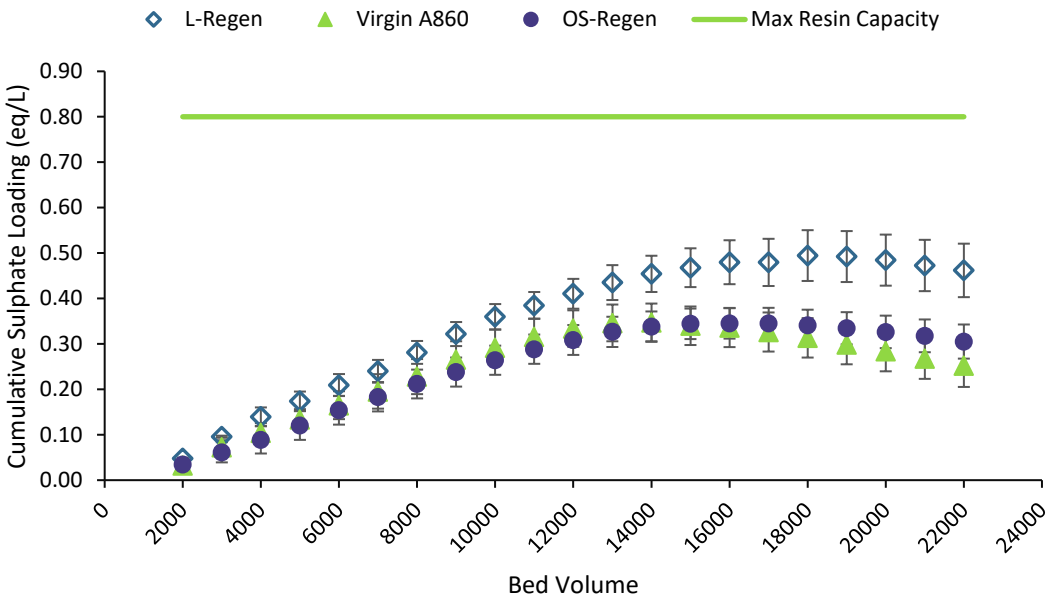

Figure 6-5: Cumulative sulphate loading for Virgin A860 resins, in-lab regenerated February 16th resins (L-Regen) and on-site regenerated February 17th resins (OS-Regen).

The maximum sulphate loaded onto the L-Regen resins was 0.49 ± 0.06 eq/L, while the vA860 and OS-Regen had a maximum sulphate loading of 0.35 ± 0.04 eq/L and 0.35 ± 0.03 eq/L, respectively. On performing an Aspen-Welch t-test, there was significance between the sulphate loaded on the vA860 and the L-Regen resins, as well as between the OS-Regen and the L-Regen resins with 95% confidence. There was no difference found between the vA860 and the OS-Regen. This suggests that there was significantly more sulphate loaded onto the L-Regen resins as compared to the vA860 and the OS-Regen resins. As sulphate displaces both chloride and NOM fractions during primary IEX, it is possible that the vA860 and the OS-Regen adsorbed DOC preferentially over sulphate and could have removed more DOC than the L-Regen. This would be significant as it would suggest agreement with Zimmermann et al. that the loading of sulphate has a detrimental effect on the overall DOC removal. However, because experiments

were not taken to exhaustion of secondary IEX, is it not possible to confirm if the increased sulphate loaded onto the L-Regen resins would be detrimental to total DOC removed.

6.2.3 Resin Saturation

Figure 6-6 shows the cumulative anions loaded for the June 6th, 2020, September 10th, 2020, and February 16th, 2021, resins, with starting values assumed to be zero, excluding chloride. This assumption means that the total saturation will not reach the theoretical maximum capacity of 0.8 eq/L but instead shows a summary of the remaining capacity on the resins at time of extraction.

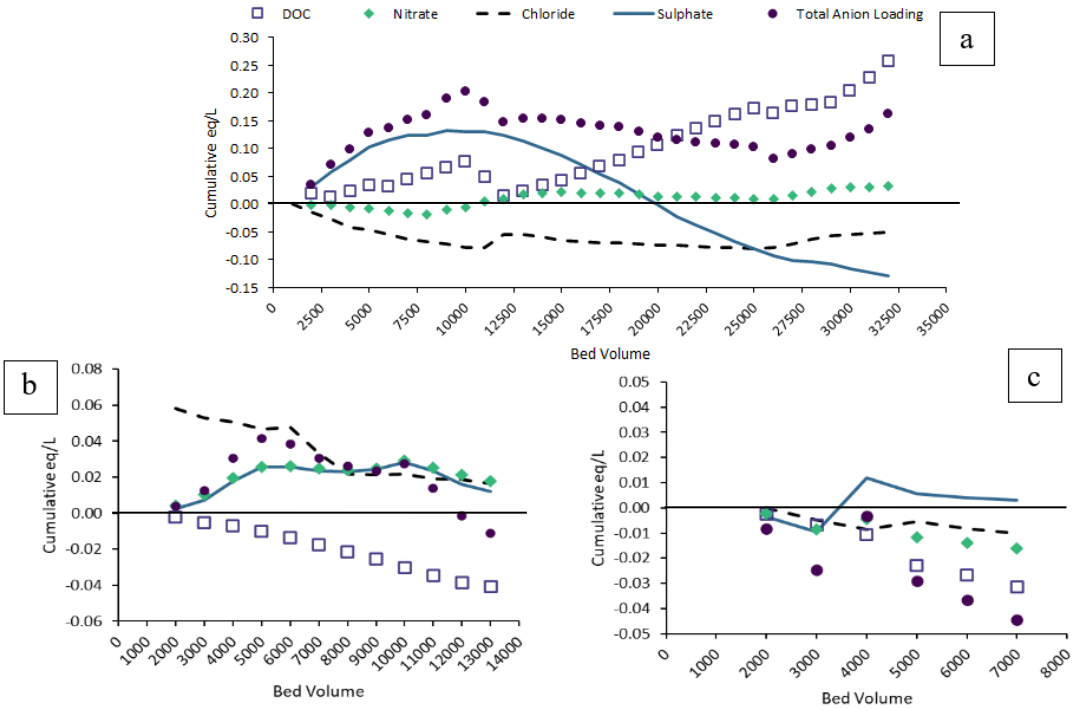

Figure 6-6: Resin saturation for a) June 2020, b) September 2020, and c) February 2021, extracted resins. The total anion loading is based on DOC, nitrate, and sulphate, assuming negligible chloride release.

As mentioned in section 6.2.2, the June resins adsorbed an additional 0.13 ± 0.5 eq/L of sulphate, seen in Figure 6-6a, while the pilot resins absorbed an estimated 0.14 eq/L total sulphate. The June resins continued to adsorb DOC for the entire 32,000 BV test, aside from release at 11,000 and 12,000 BV. Primary IEX appeared to end at 9000 BV, when the sulphate loaded began to release, indicating the start of secondary IEX. These MLTs showed that chloride appeared to have 0.08 ± 0.2 eq/L loaded on the resins at time of extraction, while in the pilot study there remained approximately 0.06 eq/L. As before, this data suggests the possibility that MLTs performed on a 1 mL sample of resins extracted from a pilot-scale column may be able to predict the capacity remaining in the large column.

Nitrate loading was negligible during the June resin MLTs, with 0.03 ± 0.03 eq/L loaded by 32,000 BV. The total DOC loaded at the end of 32,000 BV was 0.26 ± 0.17 eq/L, however comparing the loading slope with what was seen in section 5.2.2, the lack of a plateau suggests that there may have been additional capacity for DOC had testing continued. As each 1000 BV test requires 1 hour of mixing, a minimum of 32 hours was required to reach this point; if maximum loading had not been reached by this time, it indicates that multiple loading tests are a time-consuming and impractical method of determining the remaining capacity available for DOC removal. Instead, MLTs might be better used to determine pilot-scale resin capacity during early post-regeneration operation to estimate extent of primary and secondary IEX exhaustion.

For the Sept resins, a negligible 0.06 ± 0.06 eq/L of chloride was released, while 0.28 ± 0.06 eq/L of sulphate was loaded, seen in Figure 6-6b. In the pilot experiment, it was estimated that 0.01 eq/L of chloride remained and there was also a slow release of 0.02 eq/L sulphate after resin extraction. It is suspected that the differing kinetics between the pilot (packed bed) and the MLT (stirred bed), as well as biofilm accumulation in the pilot column, contributed to the

additional loading of sulphate during MLTs: biofilm erosion in MLTs may have exposed sites that would potentially have remained blocked in the pilot column. The Sept results suggest that the different kinetics of MLTs may affect the ability to accurately predict the remaining sulphate available on active sites made accessible following an air scour backwash. The Feb resins showed similar results, with a negligible 0.01 ± 0.06 eq/L of chloride released and 0.01 ± 0.04 eq/L of sulphate adsorbed, seen in Figure 6-6c. The lack of meaningful data for Sept and Feb resins suggest that performing MLTs on resins close to sulphate exhaustion and during biodegradation may not provide additional information about column conditions, as without optimization of flow regime biofilm is not likely to establish during MLTs and column conditions will not be replicated (Rittmann, 1984; Winter et al., 2018).

Figure 6-7 shows the resin saturation for the virgin A860. As these resins had been freshly regenerated, it was assumed that the starting values for DOC, sulphate, and nitrate were all zero, while the chloride was set to the largest cumulative release seen during the experiment. As mentioned in section 6.2.1, the starting value for total chloride loaded was set to the maximum cumulative chloride released from the resins, assuming this value is the amount of chloride loaded and resulting in a final chloride loading of essentially zero. This assumption is likely not correct, as seen by the chloride loaded above the theoretical maximum capacity, however it showed potential error in this data cleanly as positive values above the maximum capacity, rather than as negative values. Total anions loaded summarized DOC, nitrate, and sulphate ions.

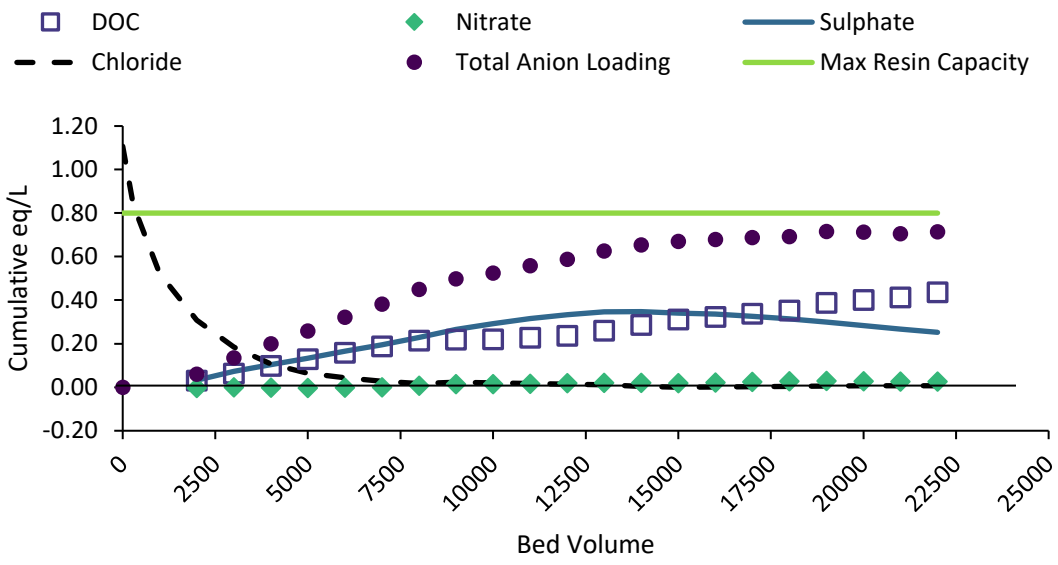

Figure 6-7: Resin saturation for regenerated virgin A860, showing loading of DOC, nitrate, sulphate, chloride, and the total anion loading.

The chloride mass balance and resulting estimate of total chloride loaded after regeneration was 1.11 ± 0.12 eq/L, above the maximum capacity of 0.8 eq/L. As mentioned in section 6.2.1, the post-regeneration rinse cycle was not as thorough as the rinse cycle performed by Zimmermann et al. (2021), which may have resulted in unbound chloride inside the pore matrix, increasing the chloride concentration in the supernatant and artificially inflating the chloride loaded (Zimmermann et al., 2021). It is suspected the total available capacity was closer to the theoretical maximum of 0.8 eq/L, as the total anions loaded began to plateau around 0.71 ± 0.09 eq/L, with the excess chloride loading likely being due to insufficient rinsing. The chloride loading data for regeneration MLTs was an unreliable estimate for total resin capacity.

Table 6-1 compares the loading of the vA860 with the pilot resins at the end of primary IEX, at the point prior to when sulphate began to release (secondary IEX).

Table 6-1: Resin Saturation at Transition to Secondary IEX for vA860 MLTs and Pilot Resins

	DOC Loaded (eq/L)	Sulphate Loaded (eq/L)	Chloride Loaded (eq/L)	DOC Removal (%)	Normalized UVA_{254} (C/C_o)	DOC Affinity
vA860	0.29 ± 0.10	0.35 ± 0.04	0.04 ± 0.16	24.1 ± 0.8	0.69 ± 0.01	0.20
Pilot Resins (May – Feb)	0.31	0.14	0.02	29.6 ± 0.0	0.37	0.40

At the end of primary IEX, the pilot resins showed greater DOC removal and removal of UV-absorbing compounds than the vA860, and the amount of sulphate loaded was less. These results agree with Zimmermann et al. (2021), who saw that an increase in influent sulphate concentration and subsequent increase in sulphate loading decreased the DOC removal by 19% (Zimmermann et al., 2021). The DOC affinity, calculated as the ratio of DOC adsorbed to DOC fed, indicated that the pilot resins had a much higher affinity for DOC than the vA860 resins used in the MLTs. Winter et al. (2018) saw similar results when comparing the DOC removal of columns and MLTs: initially, the column tests removed more DOC than the MLTs (Winter et al., 2018).

These results suggest that removal kinetics in a stirred bed increased the resin affinity for sulphate, leading to more sulphate loaded during MLTs, and possibly extending the duration of secondary IEX compared to a packed column. This phenomenon would have to be explored through kinetics experiments on the adsorption of sulphate at different conditions during MLTs. It is not expected that there would be a difference in resin capacity as Winter et al. saw no change in the equilibrium DOC (Winter et al., 2018).

Comparing the L-Regen (a) with the OS-Regen (b) in Figure 6-8, the total anions loaded at 22,000 BV was 0.75 ± 0.11 eq/L loaded and 0.63 ± 0.12 eq/L loaded, respectively.

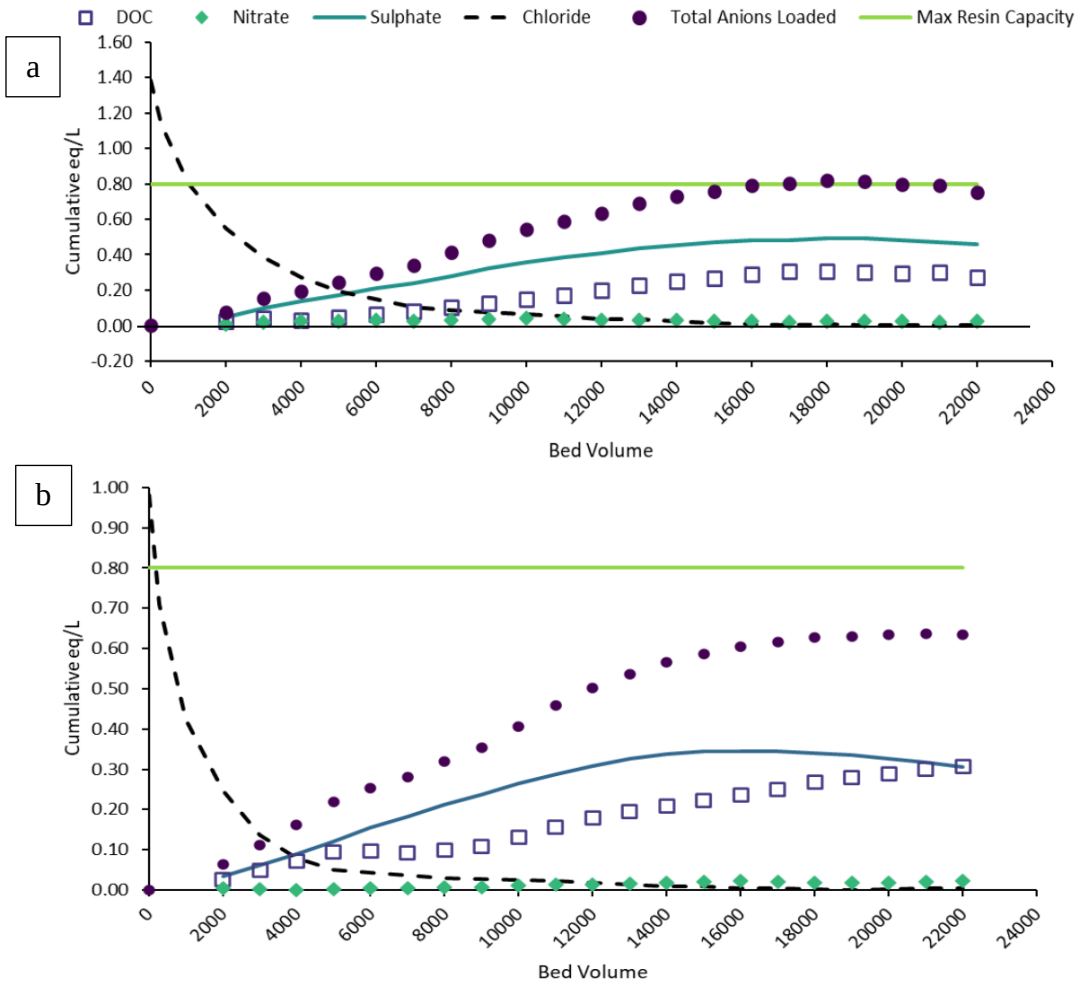

Figure 6-8: Resin saturation for a) in-lab regenerated resins (L-Regen) and b) on-site regenerated resins (OS-Regen), showing loading of DOC, nitrate, sulphate, chloride, and the total anion loading.

Cumulative error introduced uncertainty and overlap into these values, and a t-test comparing the L-Regen and OS-Regen total anions loaded averages showed no difference at 95% confidence. This suggests that, despite differing regeneration kinetics (the L-Regen resins were regenerated in a stirred bed in the lab versus the OS-Regen resins which were regenerated in a packed bed on

site), the total capacity available for ion exchange was the same, as suggested by Winter et al. (Winter et al., 2018). Table 6-2 summarizes and compares the anions loaded and the removal efficiency as normalized UVA_{254} at transition to secondary IEX, and the final cumulative anions loaded for the L-Regen, OS-Regen, and the pilot resins after the February regeneration.

Table 6-2: Resin Saturation at Transition to Secondary IEX for L-Regen, OS-Regen, and Pilot Resins.

	DOC Loaded (eq/L)	Sulphate Loaded (eq/L)	Chloride Loaded (eq/L)	Norm. UVA_{254} (C/C_o)	DOC Affinity	Final Cum. Anions Loaded (eq/L)
L-Regen	0.30 ± 0.03	0.49 ± 0.06	0.01 ± 0.42	0.72 ± 0.01	0.16	0.75 ± 0.11
OS-Regen	0.24 ± 0.07	0.35 ± 0.03	0.01 ± 0.14	0.80 ± 0.01	0.14	0.63 ± 0.12
Pilot Resins (Feb – Aug)	0.21	0.18	0.01	0.36	0.66	0.43

Comparing the DOC affinity, it is clear to see that the resins in the pilot column had a higher DOC affinity than the resins used in MLTs, as was also seen in the comparison in Table 6-1 between the vA860 and the pilot resins. At this point, the OS-Regen resins were being outperformed by the L-Regen resins; despite removing similar eq/L of DOC, the L-Regen resins had better removal of UV-absorbing compounds while also removing more sulphate. The increased performance of the L-Regen resins was likely due to effects of biofilm as described in section 6.1.1: regeneration in a stirred bed would not have been hindered by channelling, and biofilm erosion would have been more likely to occur during MLTs than in a packed bed, potentially exposing additional exchange sites for regeneration and subsequent IEX.

There also appeared to be a large difference in the total cumulated anions loaded between the OS-Regen and the pilot resins. Biofilm blocking the resin pore matrix may have played a large part in the apparent decreased capacity of the pilot resins. While air scour backwash may

have been successful in breaking up resin masses formed due to channelling and reducing biofilm on the resins prior to regeneration, the next air scour backwash took place almost 3 months later. Three months of biofilm growth could have resulted in pore blockage that was not remedied by the regular air scour backwashing that took place during the next 16 weeks. This potential pore blockage would have had a significant effect on IEX efficacy in the packed bed on site as compared to IEX in a stirred bed. Although the extent of biofilm growth during MLT conditions are unknown, these MLTs were only run for 22,000 BV (22 hours) and it is not expected that significant biofilm growth would have occurred without longer run times and optimization of flow regimes (Rittmann, 1984; Winter et al., 2018).

In addition to differing impacts due to biofilm, it is possible that resin loss contributed to the low capacity seen from the pilot resins. Calculations assumed that the resin volume stayed constant throughout the pilot study due to negligible volume loss from extracted aliquots of resin, however this assumption may not have been valid as losses were also incurred from air scouring and maintenance. The accuracy of bed height measurements would also be affected by bed compaction, resin swelling, uneven settling, and misreading due to the measuring method; the bed height was measured by shining a light behind the column and measuring the shadow height, assumed to be the resin bed. A loss of only 5 L would result in an increased estimated pilot resin capacity of 0.51 eq/L from 0.43 eq/L, which is within the error of final anion accumulation of the OS-Resin MLTs. Future pilot experiments should establish a more accurate method of bed volume measurements to properly assess starting bed volume and account for the changes over time.

Chapter 7: Conclusions and Recommendations

To explore the efficacy of IEX and BIEX in treating surface water with high concentrations of DOC, pilot- and laboratory-scale experiments were performed. The majority of the research for this work occurred on site at Gillies Bay Improvement District, where a pilot system operated for 466 days, with additional supporting laboratory experiments. Key findings are as follows:

- The BIEX column removed >50% DOC for approximately 58 days (until Aug. 2020), at a 10 min EBCT, during which primary and secondary IEX were the main mechanisms of DOC removal. Secondary IEX continued until Sept. 2020, after which biodegradation was assumed to be the only mechanism removing DOC. After regeneration on February 17th, 2021, the BIEX column removed >50% DOC continuously until April 14th, and for a total of 73 days with air scour backwash implemented at a 20 min EBCT.

- Introducing air scouring into the backwash procedure likely exposed sites blocked by biofilm or resin aggregation, thereby allowing for extension of the filter life in secondary IEX through increased access to loaded sulphate ions. The result of implementing regular air scour backwashing to column maintenance and increasing the EBCT was an increase in the number of days with > 50% DOC removal from 58 to 73 days and doubled the operational life (defined here as start of primary IEX to end of secondary IEX) of the filter from 82 days to 169 days.

- The total anion balance (sum of anions loaded/sum of anions released) for primary and secondary IEX was 0.83 and 0.95, respectively, between February and August 2021, as compared to 0.93 reported by Zimmermann et al. and ~ 0.4 reported by Edgar & Boyer (Edgar & Boyer, 2021; Zimmermann et al., 2021).

Addressing the hypotheses proposed in section 3.2:

- Hypothesis 1 proposed the possibility of 9 months of >50% DOC removal and was proven to be false. Water with an initial DOC concentration of 9 mg/L was treated by BIEX and achieved a 50% DOC removal for 58 days (~ 2 months) without air scour backwash, and 73 days (~2.5 months) with air scour backwash.

- Hypothesis 2 proposed that multiple cycles of BIEX to biodegradation may decrease the overall resin capacity. This was unable to be addressed in full due to only one instance of BIEX operating beyond secondary IEX exhaustion. Instead, multiple loading tests showed that it may be possible to predict total resin capacity available for IEX at pilot scale using extracted resin aliquots. MLTs also showed that the effects of biofilm growth inside a pilot column may affect usable resin capacity through pore matrix blocking.

7.1 Significance of Work

This research was undertaken to expand on the knowledge of BIEX as a water treatment technology for the removal of DOC from surface water. Compared with previous pilot work, this research showed that a higher DOC concentration impacted the operating time that BIEX could remove > 50% DOC. The implementation of air scour backwash was seen to double the operational life of the BIEX filter, which would reduce the time between regenerations and decrease the service requirements; however, this strategy would require the addition of air compressors. For a small community, the increase in filter life would reduce regeneration frequencies and chemical consumption, yet the addition of air compressors introduce further complexity to a system, are another source of required maintenance and repair, and are a noise hazard. This work also showed that primary and secondary IEX provided the bulk of DOC removal, while biological degradation had a lower contribution in line with BAC DOC removal, as seen by the anion balance. The primary and secondary IEX anion balance showed a 0.91:1 ratio of anions loaded to released, while after secondary IEX had exhausted the anion balance was 1.1:1, an indication of biodegradation. The knowledge gained through this research into the efficacy of BIEX for Cranby Lake water, the implications of air scour backwash on extension of filter life, and the understanding that the bulk DOC removal occurs in primary and secondary IEX along with the data collected, will be used to help the community of Gillies Bay Improvement District develop a new water treatment system.

7.2 Future Work Recommendations

There is much work that could be undertaken to further knowledge of BIEX:

- Air scour backwash:
    - Investigate the impact of air scouring on biofilm growth and erosion
    - Optimization of air scouring procedures could maximize access to blocked sites

- Sulphate regeneration:
    - Explore the trade-off between potential cost decrease and reduction in efficiency alongside lower environmental toxicity
    - Investigate benefits of air scour backwashing in sulphate-regenerated systems

- Biological activity
    - Investigate the biofilm microbial community to determine mechanisms of biodegradation and possible nitrification
    - Compare microbial communities arising from different water sources to understand common microorganisms participating in biodegradation
    - Investigate if a seeded microbial community could survive and impact biodegradation efficiency

References

Alkan, U., Teksoy, A., Ateşli, A., & Başkaya, H. S. (2007). Influence of humic substances on the ultraviolet disinfection of surface waters. *Water and Environment Journal*, *21*(1), 61–68. https://doi.org/10.1111/j.1747-6593.2006.00047.x

Amini, N., Papineau, I., Storck, V., Bérubé, P. R., Mohseni, M., & Barbeau, B. (2018). Long-term performance of biological ion exchange for the removal of natural organic matter and ammonia from surface waters. *Water Research*, *146*, 1–9. https://doi.org/10.1016/j.watres.2018.07.057

Ates, N., & Incetan, F. B. (2013). Competition impact of sulfate on NOM removal by anion-exchange resins in high-sulfate and low-SUVA waters. *Industrial and Engineering Chemistry Research*, *52*(39), 14261–14269. https://doi.org/10.1021/ie401814v

Baird, Rodger B., Eaton, Andrew D., Rice, E. W. (Ed.). (2017). *Standard Methods: For the Examination of Water and Wastewater* (23rd ed.). https://doi.org/10.1016/0003-2697(90)90598-4

Bazri, M. M., Barbeau, B., & Mohseni, M. (2016). Evaluation of Weak and Strong Basic Anion Exchange Resins for NOM Removal. *Journal of Environmental Engineering (United States)*, *142*(10), 1–8. https://doi.org/10.1061/(ASCE)EE.1943-7870.0001111

Bazri, M. M., Martijn, B., Kroesbergen, J., & Mohseni, M. (2016). Impact of anionic ion exchange resins on NOM fractions: Effect on N-DBPs and C-DBPs precursors. *Chemosphere*, *144*, 1988–1995. https://doi.org/10.1016/j.chemosphere.2015.10.086

Bazri, M. M., & Mohseni, M. (2016). Impact of natural organic matter properties on the kinetics of suspended ion exchange process. *Water Research*, *91*, 147–155. https://doi.org/10.1016/j.watres.2015.12.036

Bolto, B., & Dixon, D. (2002). Removal of natural organic matter by ion exchange. *Water Resear*, *36*, 5057–5056. https://doi.org/10.1021/es071940n

Bolto, B., Dixon, D., Eldridge, R., & King, S. (2002). Removal of THM precursors by coagulation or ion exchange. *Water Research*, *36*(20), 5066–5073. https://doi.org/10.1016/S0043-1354(02)00232-4

Buchanan, W., Roddick, F., & Porter, N. (2008). Removal of VUV pre-treated natural organic matter by biologically activated carbon columns. *Water Research*, *42*(13), 3335–3342. https://doi.org/10.1016/j.watres.2008.04.014

Cantor, K. P., Lynch, C. F., Hildesheim, M. E., Dosemeci, M., Lubin, J., Alvanja, M., & Craun, G. (1997). *Drinking Water Source and Chlorination Byproducts I. Risk of Bladder Cancer* (pp. 21–29). pp. 21–29. Bethesda, MD: Epidemiology Resources Inc.

Chang, H. T., Rittmann, B. E., Amar, D., Heim, R., Ehlinger, O., & Lesty, Y. (1991). Biofilm detachment mechanisms in a liquid fluidized bed.pdf. *Biotechnology and Bioengineering*, *38*, 499–506.

Chen, J., Gu, B., LeBoeuf, E. J., Pan, H., & Dai, S. (2002). Spectroscopic characterization of the structural and functional properties of natural organic matter fractions. *Chemosphere*, *48*(1), 59–68. https://doi.org/10.1016/S0045-6535(02)00041-3

Cornelissen, E. R., Moreau, N., Siegers, W. G., Abrahamse, A. J., Rietveld, L. C., Grefte, A., … Wessels, L. P. (2008). Selection of anionic exchange resins for removal of natural organic matter (NOM) fractions. *Water Research*, *42*(1–2), 413–423. https://doi.org/10.1016/j.watres.2007.07.033

Crittiden, J. (2012). *MHW´s Water Treatment*.

Dixit, F. (2017). *Anion exchange resins for the removal of microcystins from surface water*. Retrieved from https://circle.ubc.ca/

Edgar, M., & Boyer, T. H. (2021). Removal of natural organic matter by ion exchange: Comparing regenerated and non-regenerated columns. *Water Research*, *189*, 116661. https://doi.org/10.1016/j.watres.2020.116661

Gari-Grulovic, R., Bokovi-Vragolovi, N., Grbavi, E., & Pjanovi, R. (2011). Hydrodynamics and Mass Transfer in Heterogeneous Systems. In *Advanced Topics in Mass Transfer*. https://doi.org/10.5772/14587

Gibert, O., Lefèvre, B., Fernández, M., Bernat, X., Paraira, M., Calderer, M., & Martínez-Lladó, X. (2013). Characterising biofilm development on granular activated carbon used for drinking water production. *Water Research*, *47*(3), 1101–1110. https://doi.org/10.1016/j.watres.2012.11.026

Golub, L. L. (1957). *Kinetic Studies with Ion Exchange Resin Catalysts*.

Government of Canada. (2020). Drinking water advisories by community size. Retrieved from https://www.canada.ca/en/environment-climate-change/services/environmental-indicators/drinking-water-advisories.html

Government of Canada. (2021). Remaining long-term drinking water advisories. Retrieved August 27, 2021, from https://www.sac-isc.gc.ca/eng/1614387410146/1614387435325

Jarusutthirak, C., & Amy, G. (2007). Understanding soluble microbial products (SMP) as a component of effluent organic matter (EfOM). *Water Research*, *41*(12), 2787–2793. https://doi.org/10.1016/j.watres.2007.03.005

Kramer, M. D., Lynch, C. F., Isacson, P., & Hanson, J. W. (1992). The association of waterborne chloroform with intrauterine growth retardation. *Epidemiology*, *3*(5), 407–413. https://doi.org/10.1097/00001648-199209000-00005

Li, Q., Yu, S., Li, L., Liu, G., Gu, X., Liu, M., … Ren, L. (2017). Microbial communities shaped by treatment processes in a drinking water treatment pland and their contribution and threat to drinking water safety. *Frontiers in Microbiology*, *8*. Retrieved from https://www.frontiersin.org/article/10.3389/fmicb.2017.02465

Liu, Z., Lompe, K. M., Mohseni, M., Bérubé, P. R., Sauvé, S., & Barbeau, B. (2020). Biological ion exchange as an alternative to biological activated carbon for drinking water treatment. *Water Research*, *168*. https://doi.org/10.1016/j.watres.2019.115148

Liu, Z., Mills, E. C., Mohseni, M., Barbeau, B., & Bérubé, P. R. (2022). Biological ion exchange as an alternative to biological activated carbon for natural organic matter removal: Impact of temperature and empty bed contact time (EBCT). *Chemosphere*, *288*. https://doi.org/10.1016/j.chemosphere.2021.132466

Lu, Z., Sun, W., Li, C., Cao, W., Jing, Z., Li, S., … Liu, S. (2020). Effect of granular activated carbon pore-size distribution on biological activated carbon filter performance. *Water Research*, *177*, 115768. https://doi.org/10.1016/j.watres.2020.115768

Ma, H., Allen, H. E., & Yin, Y. (2001). Characterization of isolated fractions of dissolved organic matter from natural waters and a wastewater effluent. *Water Research*, *35*(4), 985–996. https://doi.org/10.1016/S0043-1354(00)00350-X

Nicolella, C., Chiarle, S., Di Felice, R., & Rovatti, M. (1997). Mechanisms of biofilm detachmend in fluidized bed reactors.pdf. *Water and Science Technology*, *36*(1), 229–235.

Purolite. (2021). Purolite A860. Retrieved from https://www.purolite.com/product/a860

Ritchie, J. D., & Michael Perdue, E. (2003). Proton-binding study of standard and reference fulvic acids, humic acids, and natural organic matter. *Geochimica et Cosmochimica Acta*, *67*(1), 85–96. https://doi.org/10.1016/S0016-7037(02)01044-X

Rittmann, B. E. (1984). Comparative performance of biofilm reactor types. *Biotechnology and Bioengineering*, *26*(9), 1139–1139. https://doi.org/10.1002/bit.260260922

Rittmann, B. E., & McCarty, P. L. (2001). *Environmental Biotechnology : Principles and Applications* (Vol. 7). Retrieved from http://www.sciencedirect.com/science/article/pii/S0958166996800474

Roberts, P. V., & Summers, R. S. (1982). Performance of granular activated carbon for total organic carbon removal. *Journal / American Water Works Association*, *74*(2), 113–118. https://doi.org/10.1002/j.1551-8833.1982.tb04858.x

Schulz, M., Winter, J., Wray, H., Barbeau, B., & Bérubé, P. (2017). Biologically active ion exchange (BIEX) for NOM removal and membrane fouling prevention. *Water Science and Technology: Water Supply*, *17*(4), 1178–1184. https://doi.org/10.2166/ws.2017.016

Schwanke, A. J., Balzer, R., & Pergher, S. (2019). Microporous and mesoporous materials from natural and inexpensive sources. *Handbook of Ecomaterials*, *5*, 3379–3399. https://doi.org/10.1007/978-3-319-68255-6_43

Servais, P. (1995). *BIOLOGICAL COLONIZATION OF GRANULAR Granular-activated-carbon (GAC) filters have been used for 20 years to remove dissolved organic matter by adsorption . More recently , it has been shown that , in addition to adsorption of organic matter , GAC is also*. *120*(4), 888–899.

Sillanpää, M. (2015). Natural Organic Matter in Water. In *Natural Organic Matter in Water*. https://doi.org/10.1016/c2013-0-19213-6

Statistics Canada. (2022). Rural area (RA). Retrieved March 16, 2022, from Dictionary, Census of Population, 2021 website: https://www12.statcan.gc.ca/census-recensement/2021/ref/dict/az/Definition-eng.cfm?ID=geo042

Suez. (2017). *Sievers M5310 C TOC Analyzers* (p. 330). p. 330. Retrieved from www.sieversinstruments.com

Thurman, E. M. (1985). Organic Geochemistry of Natural Waters. In *Organic Geochemistry of Natural Waters*. https://doi.org/10.1007/978-94-009-5095-5

US EPA. (1974). *Method 310 . 2 : Alkalinity (Colorimetric , Automated , Methyl Orange) by Autoanalyzer*.

Villanueva, C. M., Cantor, K. P., Grimalt, J. O., Malats, N., Silverman, D., Tardon, A., … Kogevinas, M. (2007). Bladder cancer and exposure to water disinfection by-products through ingestion, bathing, showering, and swimming in pools. *American Journal of Epidemiology*, *165*(2), 148–156. https://doi.org/10.1093/aje/kwj364

WaterToday. (2021). Daily Updated Map of Canada's Boil Water Advisories. Retrieved August 27, 2021, from https://www.watertoday.ca/map-graphic.asp

Weishaar, J. L., Aiken, G. R., Bergamaschi, B. A., Fram, M. S., Fujii, R., & Mopper, K. (2003). Evaluation of specific ultraviolet absorbance as an indicator of the chemical composition and reactivity of dissolved organic carbon. *Environmental Science and Technology*, *37*(20), 4702–4708. https://doi.org/10.1021/es030360x

WHO. (2022). 12.6 Ammonia. In *Guidelines for Drinking-Water Quality* (pp. 303–306).

Winter, J., Wray, H. E., Schulz, M., Vortisch, R., Barbeau, B., & Bérubé, P. R. (2018). The impact of loading approach and biological activity on NOM removal by ion exchange resins. *Water Research*, *134*, 301–310. https://doi.org/10.1016/j.watres.2018.01.052

WSP. (2018a). Long Term Boil Water Advisory Lifted through an Innovative Approach. Retrieved

November 24, 2021, from https://www.wsp.com/en-CA/projects/village-of-middle-river-boil-water-advisory

WSP. (2018b). Long Term Boil Water Advisory Lifted through an Innovative Approach.

Yamamura, H., Kimura, K., & Watanabe, Y. (2007). Mechanism involved in the evolution of physically irreversible fouling in microfiltration and ultrafiltration membranes used for drinking water treatment. *Environmental Science and Technology*, *41*(19), 6789–6794. https://doi.org/10.1021/es0629054

Zimmermann, K., Barbeau, B., Dezfoolian, M., Cook, C., & Mohseni, M. (2020). Biological Ion Exchange Provides DOC Removal in Small Communities. *Opflow*, *46*(5), 26–29.

Zimmermann, K., Wright, J., Bérubé, P., Barbeau, B., & Mohseni, M. (2021). Biological ion exchange capable of sulphate-based secondary ion exchange during long-term DOC removal. *Water Research*, *196*, 117036. https://doi.org/10.1016/J.WATRES.2021.117036

Appendices

Appendix A Graphical Results

Supplemental graphical results for Chapter 5: and 0.

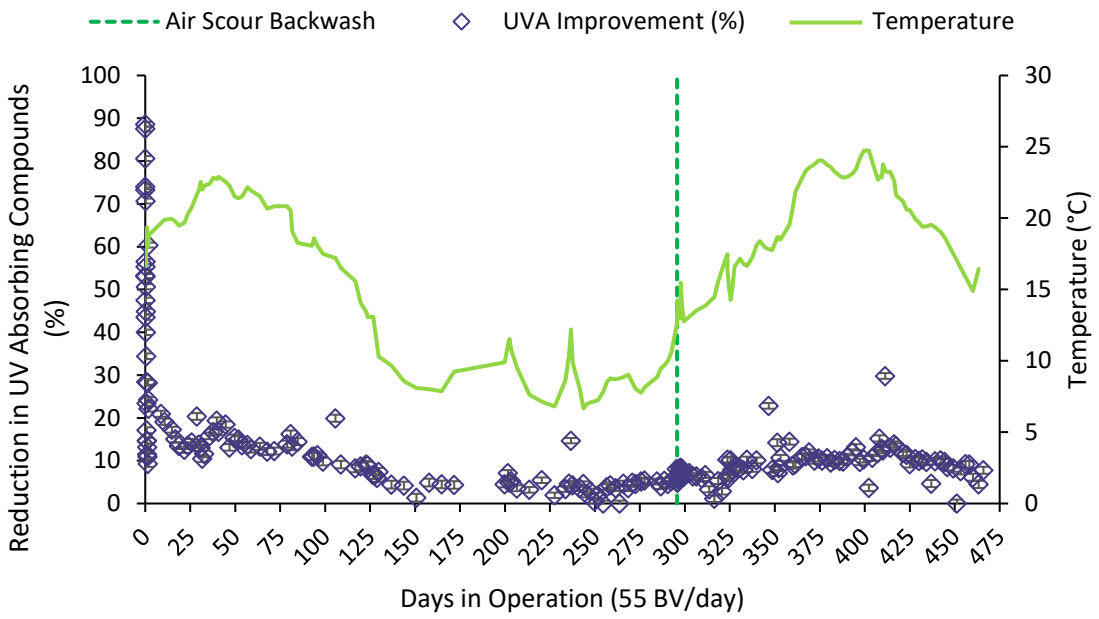

Figure A- 1: Reduction in UV-absorbing compounds for the BAC column with temperature trends over the 466-day operational life.

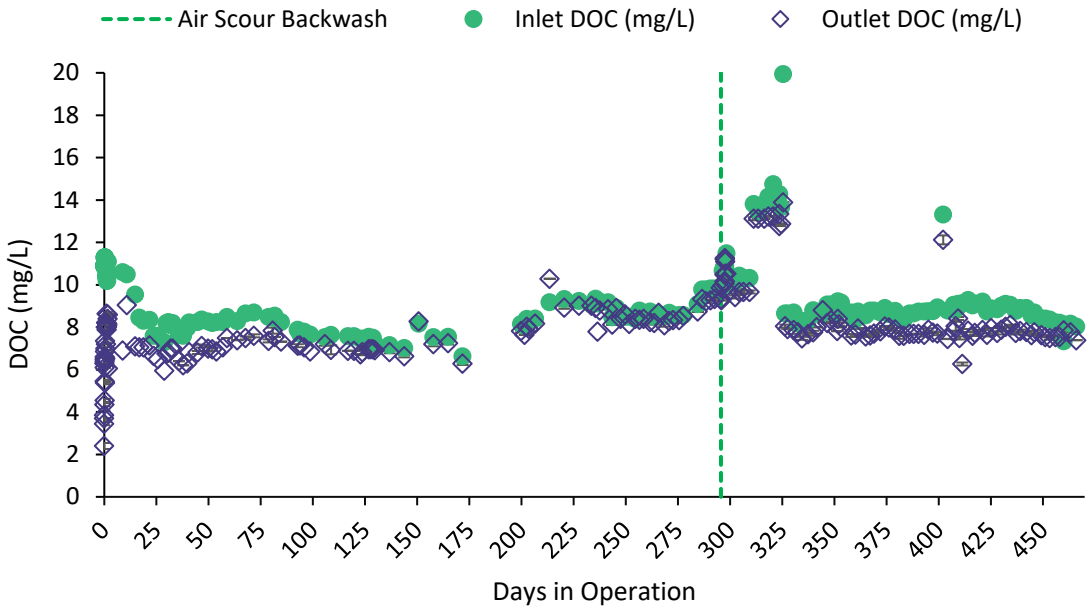

Figure A- 2: Influent and effluent DOC concentrations for the BAC column over the 466-day operational life.

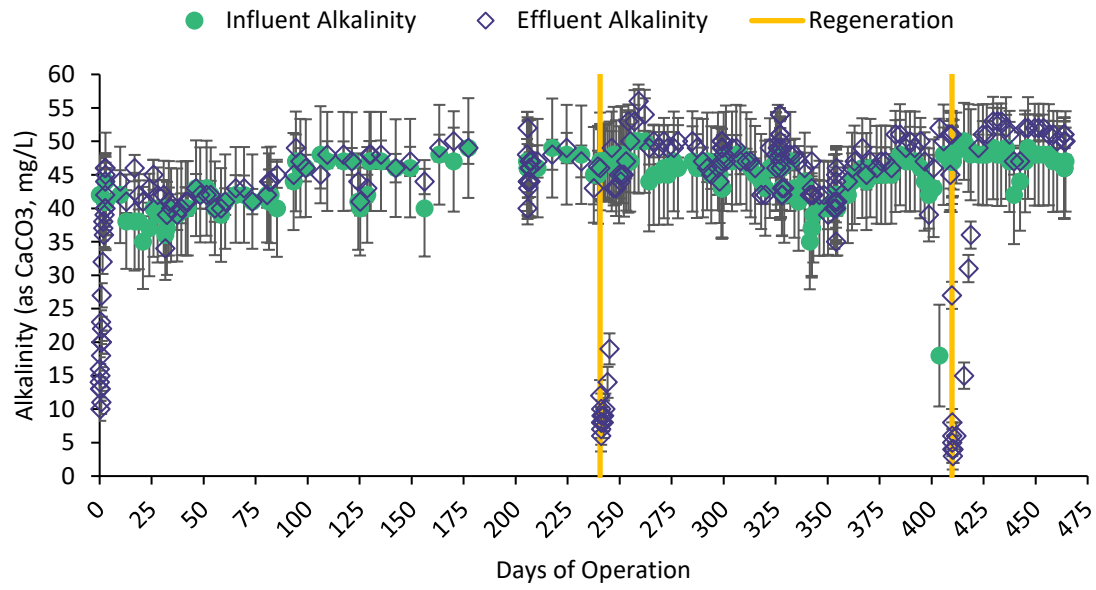

Figure A- 3: Influent and effluent alkalinity for the BIEX column over the 465-day operational life.

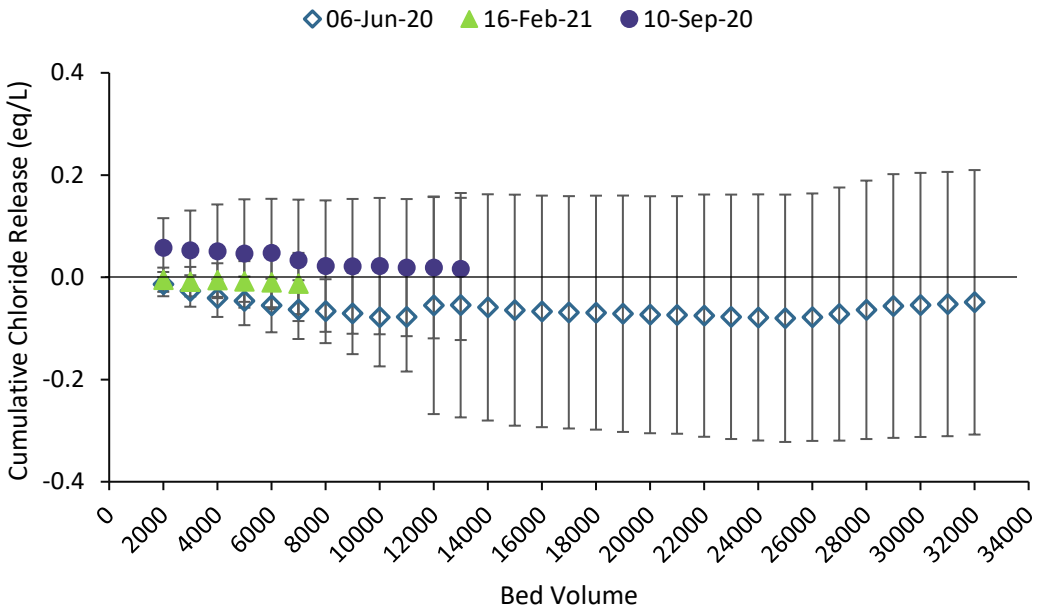

Figure A- 4: Cumulative chloride release for the June, September, and February resins.

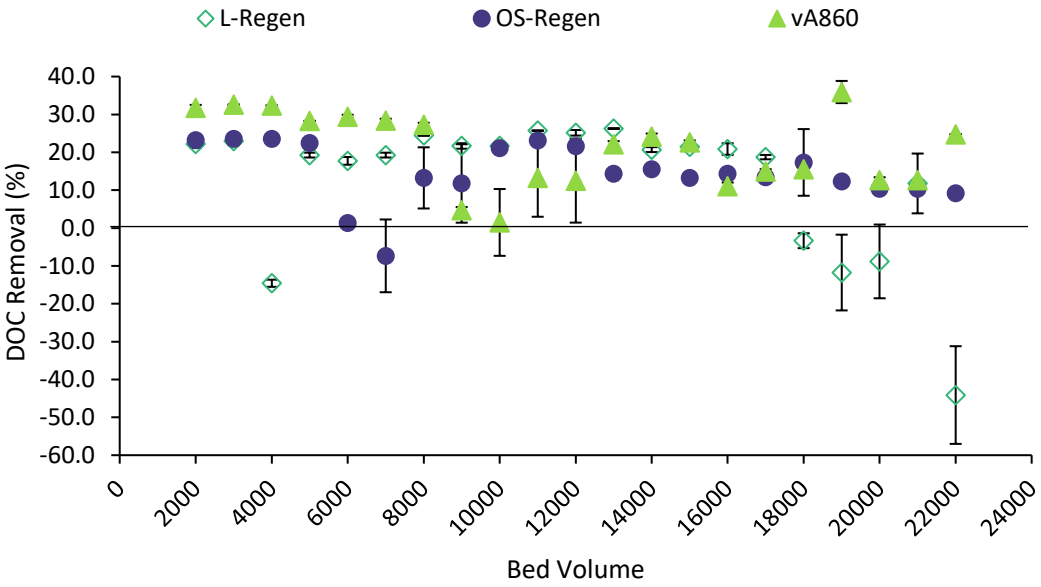

Figure A- 5: DOC removal for the February 16th in-lab regenerated resins (L-Regen), the February 17th on-site regenerated resins (OS-Regen), and the virgin A860 resins (vA860).

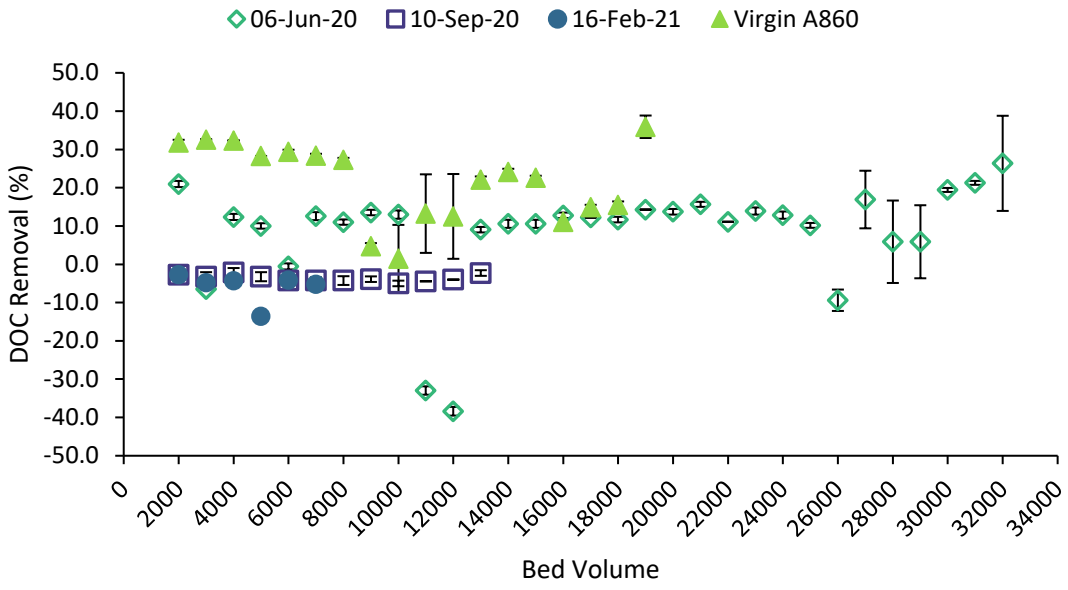

Figure A- 6: DOC removal for the June, September, and February resins compared against virgin A860.